AD-A082 183 WESTINGHOUSE DEFENSE AND ELECTRONIC SYSTEMS CENTER B--ETC F/G 17/7
INTELLIGENT TRACKING TECHNIQUES.(U)
JUL 79 T J WILLETT, J ROMANSKI, J SHIPLEY DAAK70-78-C-0167

UNCLASSIFIED NL

1 OF 2
AD
A082183

LEVEL III

(5)

INTELLIGENT TRACKING TECHNIQUES

A077869

SC

THIRD QUARTERLY REPORT

for

June 30, 1979

CONTRACT: DAAK 70-78-C-0167

Presented to

UNITED STATES ARMY

Night Vision and Electro-Optical Laboratory
Fort Belvoir, Virginia 22062

Submitted by

Westinghouse Electric Corporation
Systems Development Division
Baltimore, Maryland 21203

SECURITY CLASSIFICATION OF THIS PAGE (When Data Entered)

REPORT DOCUMENTATION PAGE

READ INSTRUCTIONS BEFORE COMPLETING FORM

1. REPORT NUMBER

2. GOVT ACCESSION NO.

3. RECIPIENT'S CATALOG NUMBER

4. TITLE (and Subtitle)
Intelligent Tracking Techniques.
Third Quarterly Report

5. TYPE OF REPORT & PERIOD COVERED
Third Quarterly Report
April 1 - June 30, 1979

6. PERFORMING ORG. REPORT NUMBER

7. AUTHOR(s)
T.J. Willett, et. al.

8. CONTRACT OR GRANT NUMBER(s)
DAAK70-78-C-0167

9. PERFORMING ORGANIZATION NAME AND ADDRESS
Systems Development Division
Westinghouse Electric Corporation
Baltimore, MD 21203

10. PROGRAM ELEMENT, PROJECT, TASK AREA & WORK UNIT NUMBERS

11. CONTROLLING OFFICE NAME AND ADDRESS
U.S. Army
Night Vision & Electro-Optical Laboratory
Fort Belvoir, Virginia 22060

12. REPORT DATE
July 30, 1979

13. NUMBER OF PAGES
93

14. MONITORING AGENCY NAME & ADDRESS (if different from Controlling Office)

15. SECURITY CLASS. (of this report)
Unclassified

15a. DECLASSIFICATION/DOWNGRADING SCHEDULE

16. DISTRIBUTION STATEMENT (of this Report)
Distribution Unlimited

17. DISTRIBUTION STATEMENT (of the abstract entered in Block 20, if different from Report)
/Willett /Romanski /Lee /Kossa Tory /Cangialosi

18. SUPPLEMENTARY NOTES

19. KEY WORDS (Continue on reverse side if necessary and identify by block number)

Automatic Target Cueing
Target Recognition
Target Tracking
FLIR Sensor
TV Sensor
Digital Image Processing
Correlation Tracker
Target Reacquisition

20. ABSTRACT (Continue on reverse side if necessary and identify by block number)

This is the Third Quarterly Report under a contract to investigate the design, test, and implementation of a set of algorithms to perform intelligent tracking and intelligent target homing on FLIR and TV imagery. The intelligent tracker will monitor the entire field of view, detect and classify targets, perform multiple target tracking and predict changes in target signature prior to the target's entry into an obscuration. The intelligent tracking and homing system will also perform target prioritization and critical aimpoint selection.

UNCLASSIFIED

SECURITY CLASSIFICATION OF THIS PAGE (When Data Entered)

405899

A system concept was developed for the intelligent tracker. A comparison was conducted between several frame-to-frame tracker designs. Work on the 875 frame storage device was completed. Seven scenarios from the NV&EOL data base were analyzed. This analysis, in conjunction with an analysis of the intelligent tracker functions, and an analysis of AAH, RPV, and PGM scenarios containing an intelligent tracker served as the basis for the system concept.

Table of Contents

INTRODUCTION

Under contract to the Army's Night Vision and Electro-Optics Laboratory, Westinghouse has been investigating the design, test, and implementation of a set of algorithms to perform intelligent tracking and intelligent target homing on FLIR and TV imagery. Research has been initiated for the development of an intelligent target tracking and homing system which will combine target cueing, target signature prediction, and target tracking techniques for near zero break lock performance. The intelligent tracker will monitor the entire field of view, detect and classify targets, perform multiple target tracking, and predict changes in target signature prior to the target's entry into an obscuration. The intelligent tracking and homing system will also perform target prioritization and critical aimpoint selection. Through the use of VLSI/VHSI techniques, the intelligent tracker (with inherent target cuer) can be applied to the fully autonomous munition.

During the third quarter, several meetings and a number of phone conversations took place between Westinghouse personnel and John Dehne and Capt. Ben Reischer of NV&EOL. A system concept was developed for the intelligent tracker. A comparison was conducted between several frame-to-frame tracker designs. Work on the 875 frame storage was completed. Seven scenarios from the NV&EOL data base were analyzed. This analysis, in conjunction with an analysis of the intelligent tracker functions, and an analysis of AAH, RPV, and PGM scenarios containing an intelligent tracker served as the basis for the system concept.

Westinghouse personnel participating in this effort include Thomas Willett, Program Manager, Dr. John Romanski, John Shipley, Leo Kossa, Tony Cangialosi, Robert Bidney, and Richard Kroupa. Program review and consultation is provided by Drs. Glenn Tisdale and Azriel Rosenfeld.

1.0 SYSTEM CONCEPT

The purpose of this section is to describe the preliminary intelligent tracker concept that has evolved from analyzing three factors: the intelligent tracker functions (described in Section 1.1 of the Second Quarterly Report); the application of the intelligent tracker to AAH, RPV, and PGM scenarios (described in Section 1.3 of the Second Quarterly Report); and seven (7) examples from the NV&EOL data base (described in Section 4.0 of this report). The functions are:

1) acquisition and handoff to tracker - locate, detect, classify, and prioritize targets automatically and handoff to a tracker (the intelligent tracker concept is assumed to include both acquisition and tracking);
2) handle multiple targets - track a number of targets in a scene simultaneously;
3) target signature prediction - predict or anticipate target occlusions and how the target signature will change as a result of the obscuration;
4) reacquisition - reacquire a target as a result of track break lock or if it leaves the field of view;
5) aimpoint selection - determine the critical aimpoint of a target, which may be an interior point within its silhouette.

A block diagram of the system concept is shown and described in terms of the first four functions. The fifth function, aimpoint selection, will be investigated in the next quarter.

1.1 SYSTEM BLOCK DIAGRAM

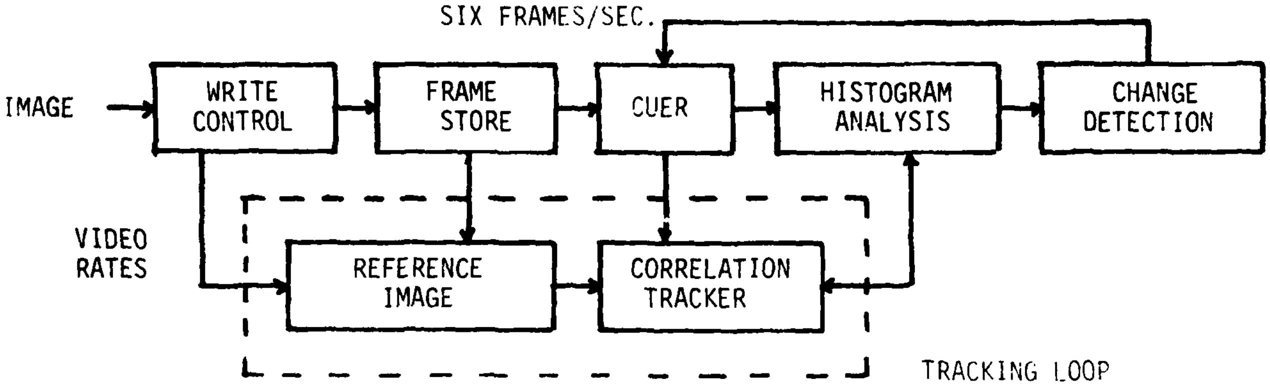

Figure 1.0-1 System Block Diagram

The system block diagram is shown in Figure 1.0-1. A timing diagram is shown in Figure 1.0-2. The horizontal line across the top of Figure 1.0-2 represents the video stream seen in one second at a video rate of 30 frames per second.

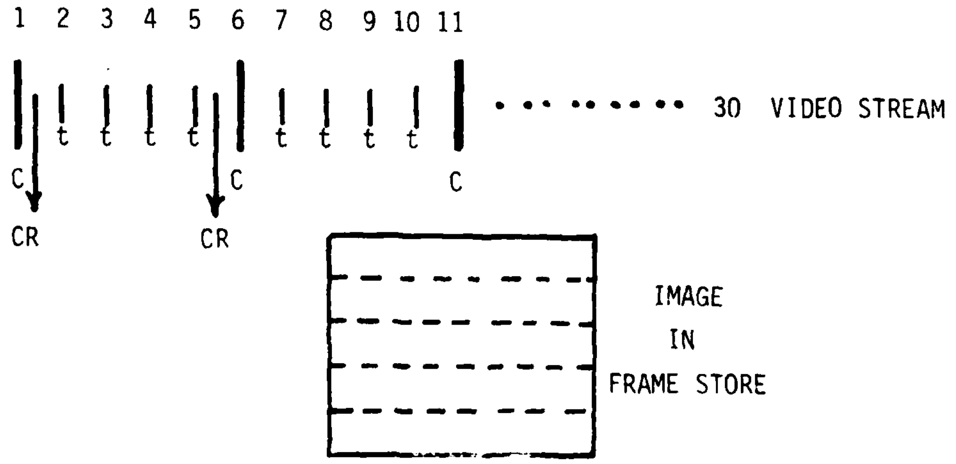

Figure 1.0-2 Timing Diagram

The heavy vertical lines represent the cued frames and the lighter vertical lines are the tracked frames. Note that there are 30 vertical lines in total. Frame 1 is a cueing frame, and frames 2,3,4, and 5 are tracking frames and then the cycle repeats. Frame 6 is a cueing frame, and frames 7,8,9, and 10 are tracking frames. The bottom of Figure 1.0-2 represents the image in the

frame store which is divided into five horizontal and addressable strips. This is done so that, instead of waiting for the entire frame to be cued before handover to tracker, targets can be handed over as soon as they are cued. The reduction in handover lag increases confidence that both cuer and tracker are working on the same target, and reduces the size of the track window. The frame store is divided into five addressable strips to aid in sending the gray level surrounding the target to the tracker for a reference image. The frame storage device is addressable in sections to increase the readout speed. It should be pointed out that the six frames per second and five strips for frame storage are approximate numbers serving as a straw man concept. The point of this discussion is that the cuer results, labelled CR, in Figure 1.0-2 can be obtained between the first and second frames instead of the fifth and sixth frames in the video stream.

Referring to Figure 1-1, we describe the handover process. A horizontal strip of a frame is snatched in real time and placed in the frame store. The cuer processes the image and detects and classifies a target. That part of the frame store holding the target and its surrounding gray scale window, assume 12 x 12 pixels for a 9 x 9 pixel target, is sent to the tracker as a reference image. The tracker converts this to a binary reference image and now tracks this target from the videostream until the next cued frame. The cuer tells the tracker where the target is within the frame so the tracker can tell the write control when to write the next target window (now from the video stream) and subsequent windows into its reference image.

For multiple target tracking, there is a reference image device for each target, but the tracker is fast enough to be multiplexed among the targets. The tracker is a bandpass binary correlation tracker (Section 2.0) in this preliminary design and the bandpass is adjusted at the cueing rate by

the cuer. Additionally, the tracker forms a smoothed track for each target in second order difference equations (to interface with the rate loop in the sensor gimbal). This allows reacquisition of a target which has left the field of view but can be brought back into view by moving the sensor along the image-centered target track.

At this point, one can imagine simultaneous multitarget cueing and tracking. The cued targets have been classified and are now ordered in an internal table in terms of priority. The priority hierarchy has been determined before the mission and loaded in the cuer. At this point in the system concept description, we have discussed the system block diagram in terms of functions 1), 2), and the first part of 4). The next topic is function 3) - target signature prediction.

To predict target obscurations, we analyze a histogram of the background ahead of the target. The track window errors, used to form the smoothed track for re-acquisition, are also used to set the histogram position. Further, the gray level reference image for the first track frame after a cued frame is also the source for the background histogram. From the histogram, we can compare the gray levels ahead of the target with that of the target. If the same gray levels are present in both, a clean target segmentation is unlikely. The target position is adjusted within the track reference window so that the tracker is using that portion of the target which will be obscured last (in the case of a target passing behind a large tree) or not obscured at all (in the case of a target passing behind some low lying shrubs). The background histogram is also analyzed for a polarity change between the target and the background. An example of this is a case where a light target against a dark background is moving into a background lighter than itself and hence becomes a dark target against a light background. Under this condition, the new background is segmented and

binary change detection at the background level is used along with direct segmentation to detect the target. Having found the front edge of the target, the tracker is switched to the front or emerging edge.

Re-acquisition resulting from track break lock is also handled by the cuer, histogram analysis, and change detection. A difficult problem here is the reappearance of a target which is partially occluded. This prevents segmentation of the entire shape so that one is forced to look for changes in the scene. The histogram analysis of the proposed target can add information because, in some of these cases, the target histogram will exhibit a peakedness not found in a background object such as a woods clearing. Otherwise, the clearing may be mistaken for a partially occluded target.

Having described the system concept in terms of a block diagram and the intelligent tracker functions, it is interesting to consider the synergism between the cuer, tracker, histogram analysis, and change detection. From a design standpoint there is a large amount of shared hardware. The binary correlation for the tracker is the same as that used by the change detection block. The histogram function forms the reference window for the tracker, forms a histogram across the target for the cuer, and forms the background histogram in the histogram analysis block. The reference frame for the tracker supplies gray levels for the background histogram analysis block. From a functional standpoint, there is also a substantial amount of synergism. Although we have referred to the tracker as a simple tracker, it is not really that simple. The cuer updates the tracker bandpass, and the histogram analysis block looks for potential obscurations. The tracker (with these aids) begins to look like the sophisticated tracker that we mentioned in the Second Quarterly Report. Further, the tracker aids in pointing out target positions to the cuer for targets cued in previous frames. This serves as a source of confirmation that both cuer and tracker are working on the same target. Finally, in a re-acquisition mode,

the cuer, histogram analysis block, change detector, and tracker work together to provide confirming information. In summary, the intelligent tracker concept has the potential of providing a substantial improvement in performance over any of its components operating alone. Further, the many shared functions and hardware offer the possibility of a smaller increase in hardware volume than anticipated.

2.0 FRAME-TO-FRAME TRACKER

In the second quarterly report, Section 3.0, we described the baseline frame-to-frame tracker and a variation called a bandpass tracker. In this section, we present a comparison between the two based on an example from the NV&EOL TV data base.

2.1 Tracker Comparison

The xy image positions of the target are shown in Figure 2-1 for successive frames 245 through 251.

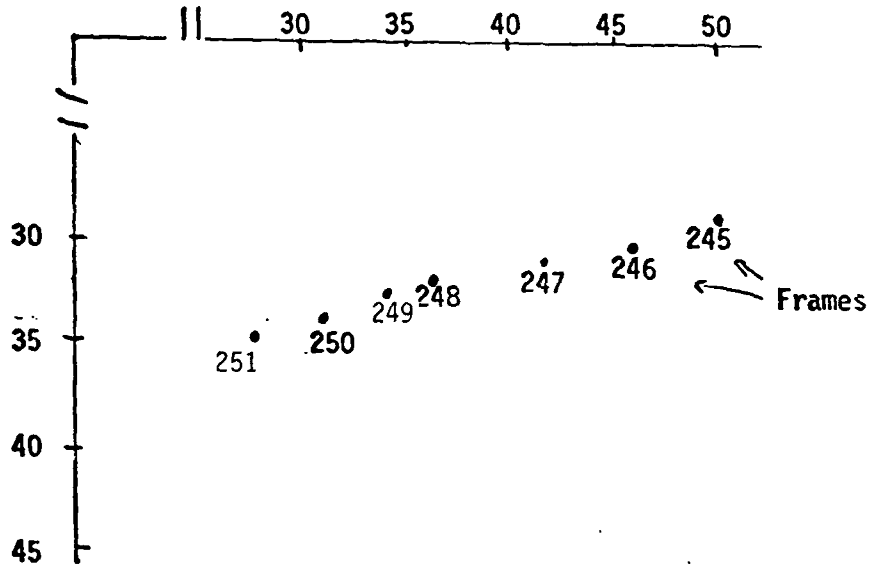

Figure 2-1. xy Target Positions

The frame-to-frame tracker is a binary correlation tracker with an inner and outer window. The inner window is initially set to cover at least 90 percent of the target. Successive tracks are established by correlating against the contents of the inner window. Section 3.0 of the Second Quarterly Report contains a detailed discussion of the tracker. The difference between the baseline tracker and the bandpass tracker is that in the latter, a range of gray levels are superposed over the inner window. This means that the target is in the inner window initially and also within a certain range of gray levels. For the comparison run, the inner window was manually placed over the target for image 245 only.

Figure 2-2 shows the gray levels of the target and its immediate background for image 245. The gray levels are coded such that numbers with a dash through them are in the twenties; numbers without a dash are in the teens, For example, the lower row is 6 which means 26; the numbers in the center of the window, representing the target are 2, 1, 3, etc. which are 12, 11, 13, and so on. Figure 2-3 shows the inner window. In the next series of figures, the baseline tracker results appear in the left or "a" figure. The bandpass tracker results appear on the right. Figures 2-4a and 2-4b show the reference images for the baseline tracker and the bandpass tracker for a threshold $t \leq 20$ for image 245.

Figures 2-5a and 2-5b shows the tracked images 245 using the same image (245) as a reference. The calculations beneath the binary image are the moment computations. Figures 2-6a and 2-6b show the tracked target for image 246 for both trackers. Note that the bandpass tracker presents a more compact target; the same situation is true for Figures 2-7a and 2-7b (image 247) and more of the target is included by the bandpass tracker. This is again true and to a greater degree in Figures 2-9a and 2-9b (image 249). Again for image 250, the addition of the lower right hand tail in Figure 2-10a would adversely affect the aimpoint computations.

```
7766555555556666
8776666555556666
7766666555555567
7766655555555566
6665541110123457
6554310886891235
5542187444779124
5431762122457914
4320762122457914
4321876223569012
4332177778990122
5553311111112222
5555544333222233
6655555544444433
6666666555555564
6666666666666666
```

Figure 2-2. Target

```
54111012
31088689
18744477
76212245
76212245
87622356
17777899
31111111
```

Figure 2-3. Bandpass, Inner Window

```
..111.1.
.1.1111.
11111111
11111111
11111111
11111111
111111..
.1111111
```

Figure 2-4a. Reference Image

```
.....1..
..111111
.1111111
11111111
11111111
11111111
.1111111
........
```

Figure 2-4b. Reference Image, t≤20

```
................
................
................
................
......111.1.....
.....1.1111.1...
....11111111.1..
...1111111111.1.
....111111111.1.
...111111111..1.
....111111...1..
.....1111111....
................
................
................
................

XBAR= 9.047
YBAR=8.719
SIG2X=89.891
SIG2Y=80.094
SIGXY=78.594
THETA=.817
```

Figure 2-5a. Tracked Image 245

```
................
................
................
................
.........1......
......111111....
.....11111111...
....1111111111..
...11111111111..
....1111111111..
.....11111111...
................
................
................
................
................

XBAR =   9.407
YBAR =   8.593
SIG2X=  95.519
SIG2Y=  76.519
SIGXY=  80.759
THETA=    .844
```

Figure 2-5b. Bandpass Tracked Image 245

```
................
................
................
................
................
................
..11111.........
.1111111........
111.111111......
1111111..1......
.11111...1......
1.....1111......
................
................
................
```

Figure 2-6a. Tracked Image 246

```
..................
..................
..................
..................
..................
..................
.111111...........
111111111.........
111111111.........
1111111111........
111111111.........
111111111.........
.11111............
..................
..................
..................
```

Figure 2-6b. Bandpass Tracked Image 246

```
................
................
................
................
................
.1111...........
.11111..........
1111111.........
11111111........
11111111........
1111111.........
111111...1......
1111....11......
......11........
................
................
```

Figure 2-7a. Tracked Image 247

```
................
................
................
................
................
.1111111........
111111111.......
1111111111......
1111111111......
11111111111.....
1111111111......
111111111.......
.111111.........
................
................
................
```

Figure 2-7b. Bandpass Tracked Image 247

```
................
................
................
................
................
................
................
...111..........
.111111.........
11111111........
111.1111.1......
111.1111..1.....
111111....1.....
11111.....1.....
........11......
11111111........
```

Figure 2-8a. Tracked Image 248

```
................
................
................
................
................
...11111........
.11111111.......
1111111111......
1111111111......
11111111111.....
11111111111.....
11111111111.....
.11111111.......
................
................
................
```

Figure 2-8b. Bandpass Tracked Image 248

```
................
................
................
................
................
................
..1.............
1..1111.........
11111111........
111111111.......
111111111.......
111111111..1....
11111111..111...
.111111...111...
........11111...
................
```

Figure 2-9a. Tracked Image 249

```
................
................
................
................
................
..1111111.......
1111111111......
11111111111.....
11111111111.....
111111111111....
11111111111.....
11111111111.....
.11111111.......
................
................
................
```

Figure 2-9b. Bandpass Tracked Image 249

```
................
................
................
................
................
................
...111..........
1111..1.........
111111.1........
...11111........
...1111.........
1111111.1.......
111111..11......
111111..11111111
1111...11111111.
.1.....11.......
```

Figure 2-10a. Tracked
Image 250

```
................
................
................
................
.111............
1111111.........
11111111........
11111111........
111111111.......
111111111.......
111111111.......
111111111.......
11111111........
.1..............
................
................
```

Figure 2-10b. Bandpass
Tracked Image 250

```
................
................
................
................
................
................
.1..............
..111111........
1111111111......
11111111111.....
111111111.1.....
111111111..1....
11111111...111..
..11111....111..
..11.....11.....
................
```

Figure 2-11a. Tracked
Image 251

```
................
................
................
................
...11111........
.111111111......
1111111111.......
11111111111.....
11111111111.....
111111111111....
111111111111....
111111111111....
.111111111.. ...
..11111.........
................
................
```

Figure 2-11b. Bandpass
Tracked Image 251

In conclusion, this set of data tends to indicate that the bandpass binary correlation tracker presents more of the target within the inner window than the binary correlation tracker without a bandpass. Further, the bandpass binary tracker presents a more compact target and a better likeness to the actual target. This not only improves track position, but allows a more accurate aimpoint selection when based on external shape. A secondary conclusion of this test is that the window width was small with regard to target motion, hence, the correlation width was not large enough, and not all the target appeared in the window.

3.0 875 LINE STORAGE DEVICE

In May, the 875 line frame snatching device completed development and was brought on line with the other pieces of the Westinghouse Image Processing Laboratory Equipment which will be used for this contract and were described in the First Quarterly Report. Figures 3.0-1 and 3.0-2 show the output of the 875 line frame grabber to a test pattern input. Figures 3.0-3 and 3.0-4 show the output for the NV&EOL data base input. The 875 line device is capable of grabbing a 125 pixel by 125 pixel window.

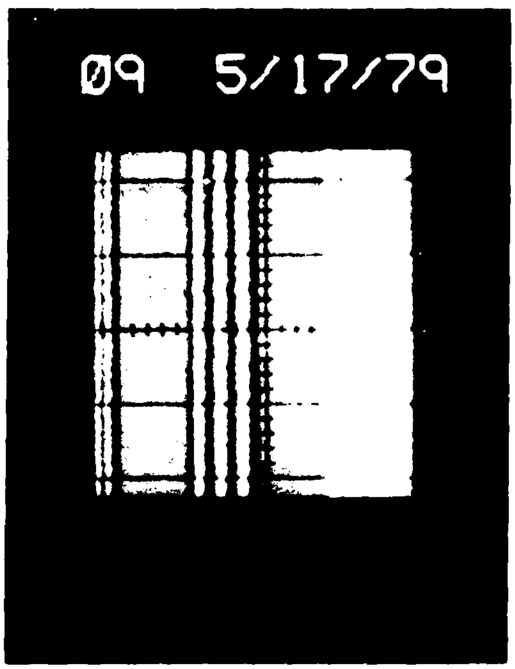

Figure 3.0-1 . Test Pattern Input

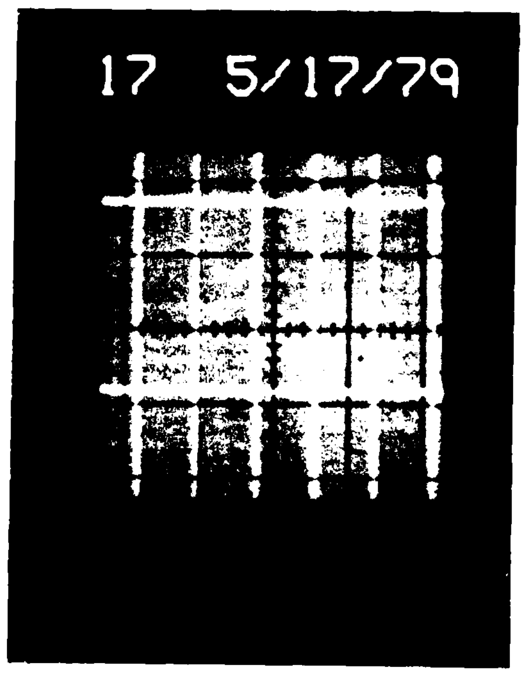

Figure 3.0-2. Test Pattern Input

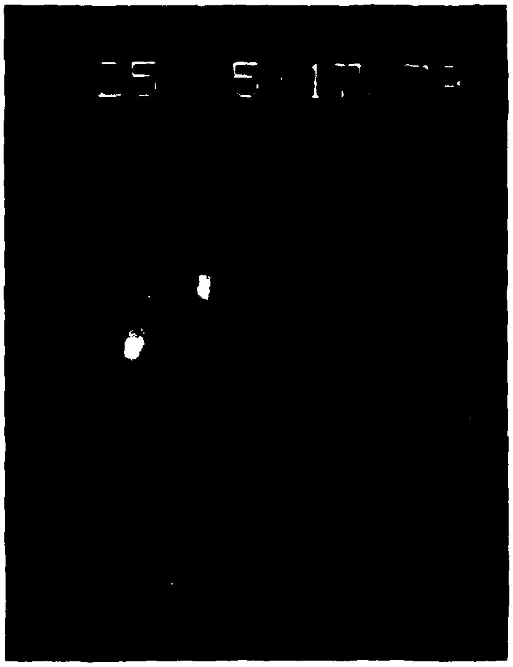

Figure 3.0-3. NV&EOL Data

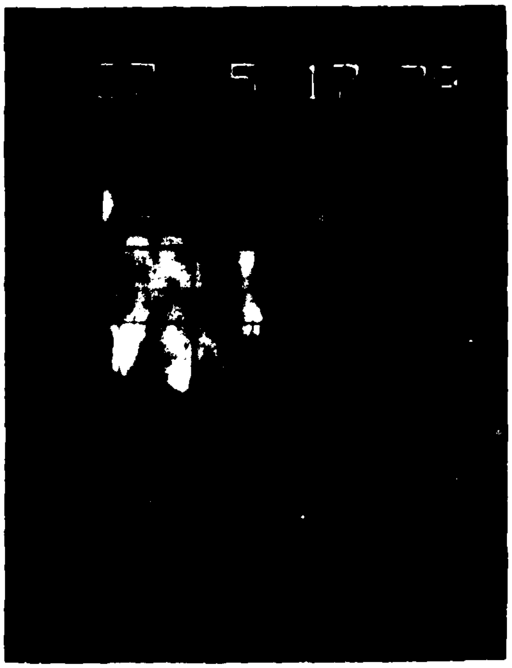

Figure 3.0-4. NV&EOL Data

This allows Westinghouse to analyze 875 line video tape data directly which will become more important as 875 line formats are used more and more by the military. Converting 875 line data to 525 line data, either through direct video tape machine conversion or through a vidicon, suffers degradation visible to the human eye.

4.0 PRELIMINARY RESULTS

This section presents seven scenarios from the NV&EOL data base in TV which was described in the Second Quarterly Report. These scenarios were analyzed with the purpose of finding methods of maintaining track and predicting obscurations. The reacquisition of a disappearing target which reappears, partially occluded, at a substantially closer range and different position is included.

4.1 Crossing Target No. 1

This set of images shows a light APC being crossed by a dark blob. The blob is associated with the sensor (SIT) such as a burn spot and is not another vehicle in the field. In one image, the blob completely covers the APC and the frame-to-frame tracker jumps to a piece of background which has gray levels within the tracker bandpass. In the next frame, the tracker jumps to another piece of background, also with the appropriate gray levels. The cuer reacquires the target as it emerges from the obscuration and redirects the tracker to the target. In summary, this scenario shows the inability of the frame-to-frame tracker to handle the case where the target is completely obscured for only a frame. Further, background is present within the track window and is at the same gray level as the tracker bandpass. This portion of the background draws the tracker. The scenario shows that the cuer-tracker combination is capable of handling such a case. Consider the scenario in some detail.

The sensor is scanning across the scene much faster than the target movement. The blob is moving toward the APC and there is negligible movement of the target against the background. The apparent movement of the blob is from right to left and diagonally down, as indicated by the dashed arrows in Figure 4.1-1.

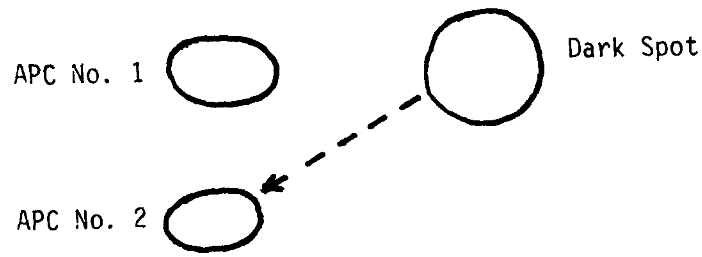

Figure 4.1-1. Target Geometry

The set of images, 287-302, is shown in Figures 4.1-2 through 4.1-17. Image 301, Figure 4.1-16, shows the APC completely obscured by the dark blob; Image 302, Figure 4.1-17 shows the APC (two small spots) emerging from the obscuration.

As an example of the interaction between cuer and tracker before the obscuration occurs, consider the cued results of image 287 shown in Figure 4.1-18. Here the maximum number of matches between perimeter points and thinned edges (See First Quarterly for a description of this segmentation process) occurs at a gray level threshold, $t \leq 16$. The APC of interest is shown in the lower left of Figure 4.1- 2. The segmented APC image is turned over to the tracker as a reference image as shown in Figure 4.1-19 and image 287 through 291 are tracked as shown in Figure 4.1-20 through 4.1-24. The tracking performance is satisfactory although the track window should have been slightly larger to account for the sensor movement, particularly evident in images 289 and 290, Figures 4.1-22 and 4.1-23. The cuer-tracker performance for the images through 299 is satisfactory and similar to that of 287-291, and need not be discussed further. We resume the analysis at image 300, just before the obscuration.

The segmented results of image 300 in Figure 4.1-25. Figure 4.1-26 shows the segmented APC as a tracker reference image and Figure 4.1-27 shows the segmented APC in image 300 as a tracked image. Figures 4.1-28 and 4.1-29

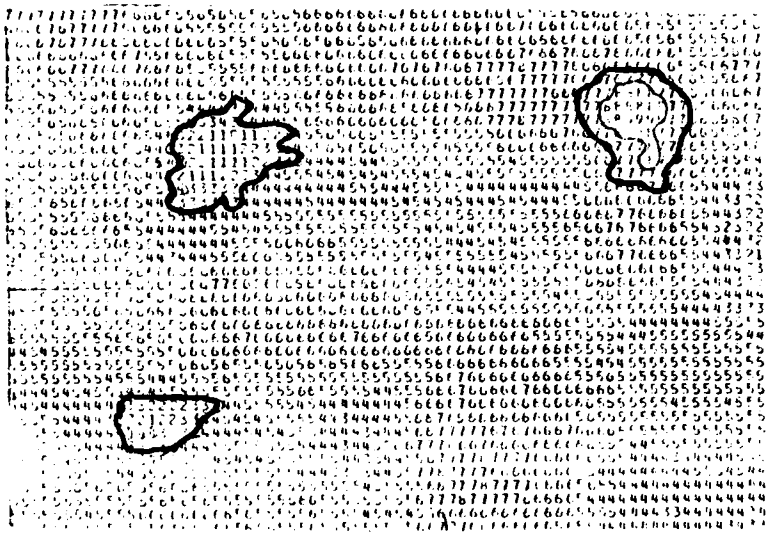

Figure 4.1-2. Image 287

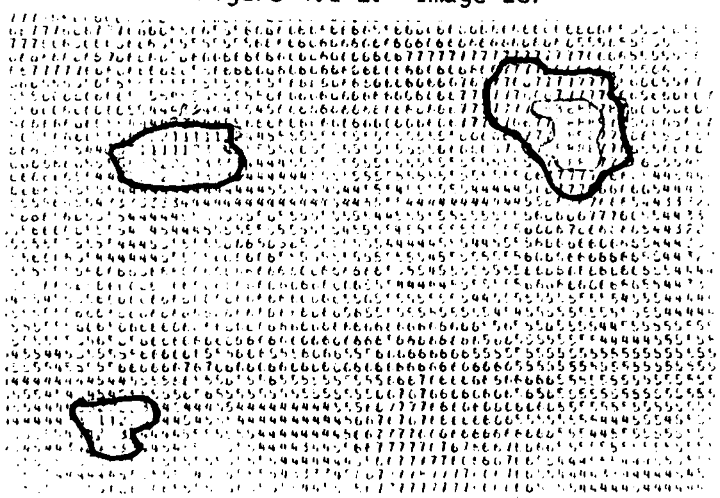

Figure 4.1-3 Image 288

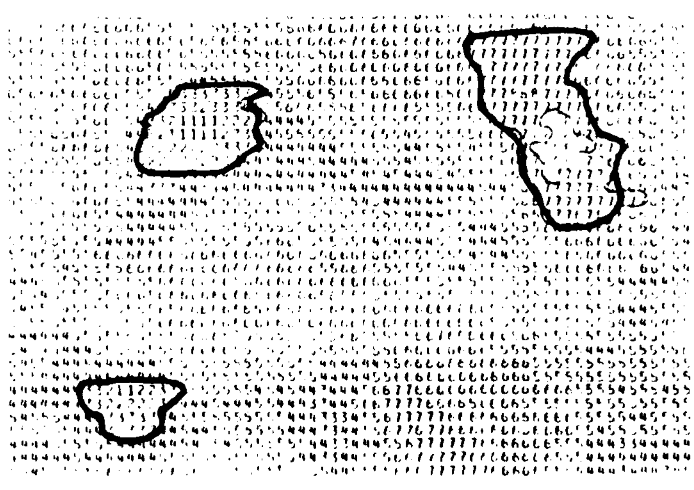

Figure 4.1-4. IMage 289

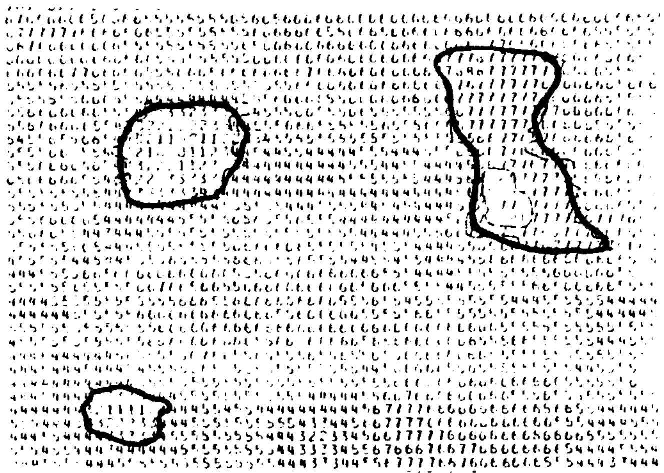

Figure 4.1-5. Image 290

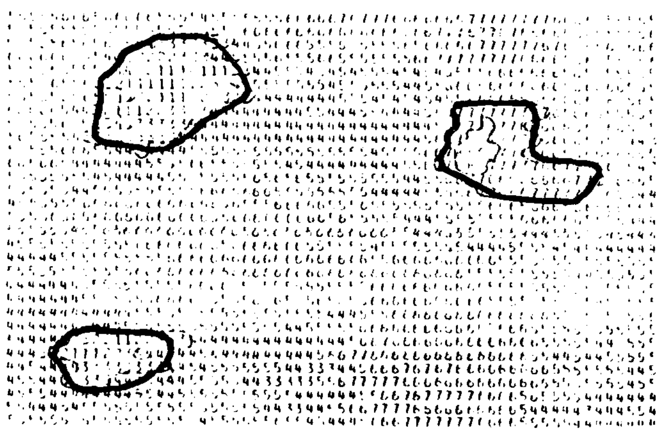

Figure 4.1-6. Image 291

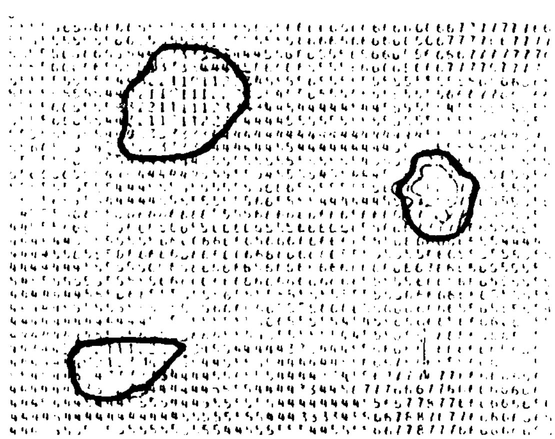

Figure 4.1-7. Image 292

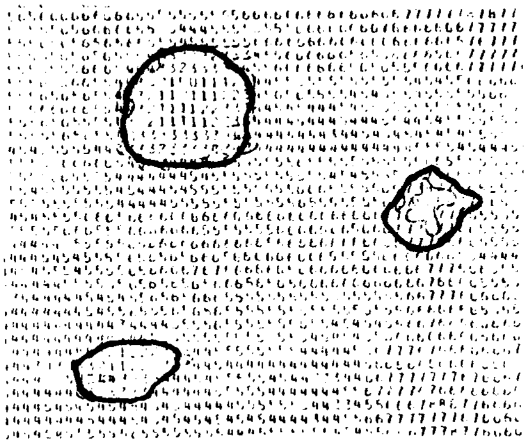

Figure 4.1-8. Image 293

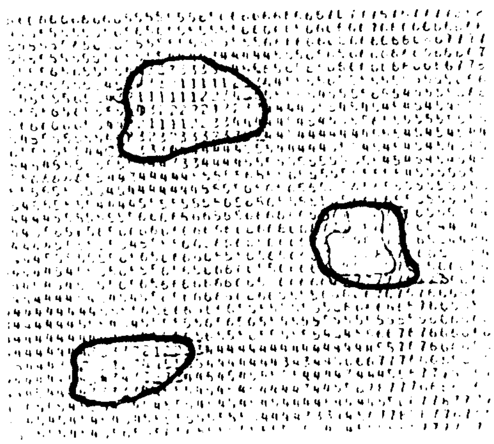

Figure 4.1-9. Image 294

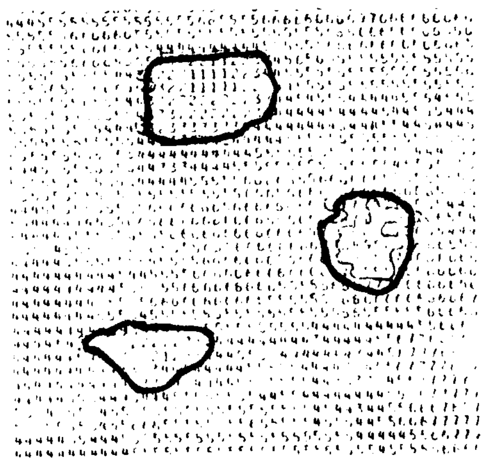

Figure 4.1-10. Image 295

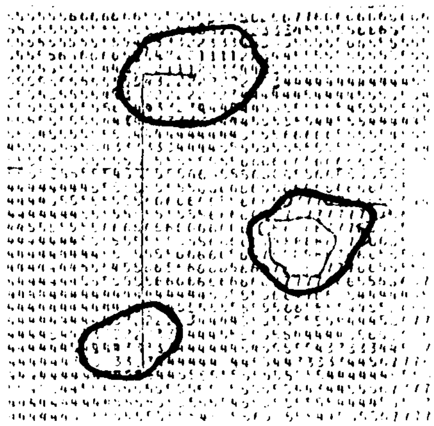

Figure 4.1-11. Image 296

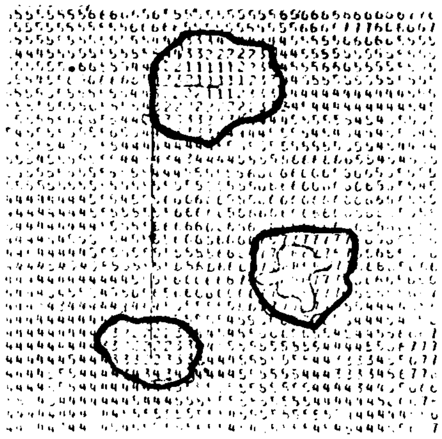

Figure 4.1-12. Image 297

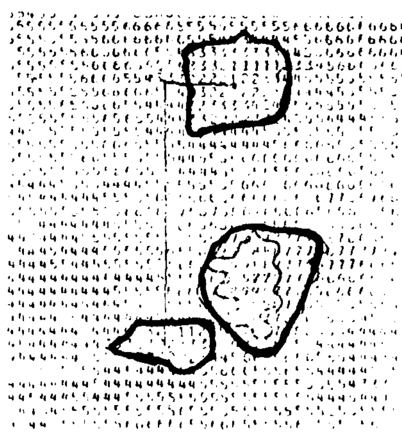

Figure 4.1-13. Image 298

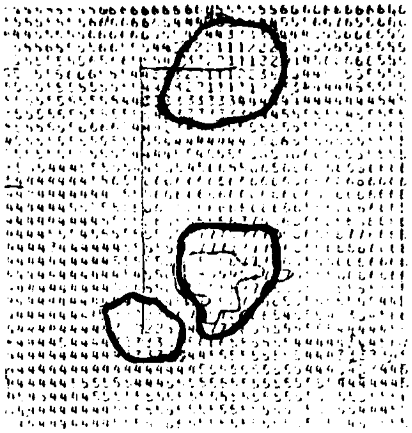

Figure 4.1-14. Image 299

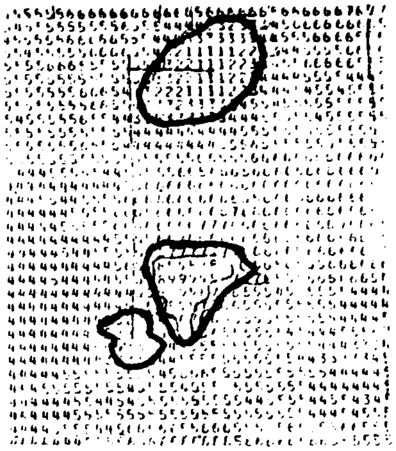

Figure 4.1-15. Image 300

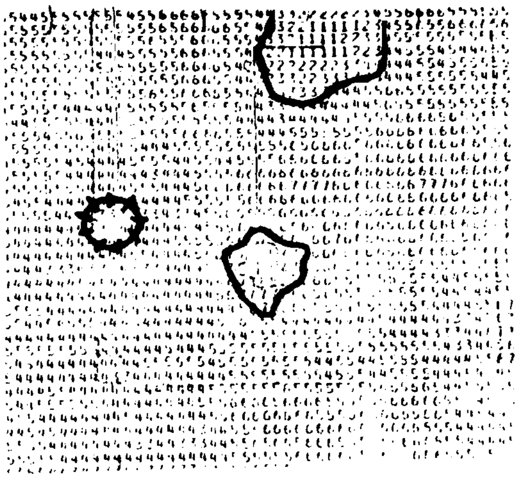

Figure 4.1-16. Image 301

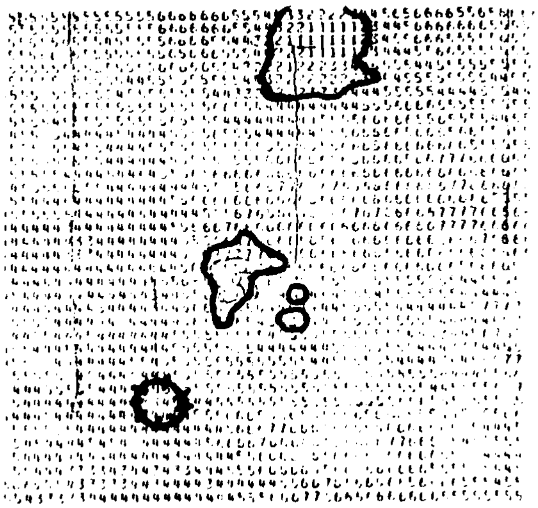

Figure 4.1-17. Image 302

```
..................
..................
..................
......1111........
....1111111.......
....1111111.......
......111.........
..................
..................
..................
```

Figure 4.1-18. Cuer Output for Image 287
(1 indicates edge/perimeter match)

```
........
........
.111111.
11111111
11111111
.111111.
........
........
```

Figure 4.1-19. Image 287,
Tracker Reference

```
................
................
................
................
................
................
.....1111111....
...1111111111...
...1111111111...
.....1111i1.....
................
................
................
................
................
................
XBAR   =   8.686
YBAR   =   8.455
SIG2X  =  80.435
```

Figure 4.1-20. Image 287

```
................
................
................
................
................
.....1111111....
.....11111111...
.....11111111...
.....1111111....
................
................
................
.................
................
................
................

XBAR   =   9.267
YBAR   =   7.500
SIG2X  =  90.600
SIG2Y  =  57.433
SIGXY  =  69.500
THETA  =    .903
```

Figure 4.1-21. Image 288

```
................
..........111...
........1111111.
.......111111111
.......111111111
........11111111
..........11111.
................
................
................
................
................
................
................
................
................
```

XBAR	=	12.220
YBAR	=	4.659
SIG2X	=	154.539
SIG2Y	=	23.829
SIGXY	=	57.341
THETA	=	1.218

Figure 4.1-22. Image 289

```
................
................
................
..........1.....
.......111111111
.......111111111
.......111111111
.........1111111
...........1111.
................
................
................
................
................
................
................
```

XBAR	=	11.564
YBAR	=	7.140
SIG2X	=	146.757
SIG2Y	=	55.863
SIGXY	=	42.532
THETA	=	1.462

Figure 4.1-23. Image 290

```
................
................
................
................
1...............
......111111....
......111111111.
.....1111111111.
......111111111.
........11111...
................
................
................
................
................
................
```

XBAR	=	10.480
YBAR	=	7.875
SIG2X	=	116.450
SIG2Y	=	63.775
SIGXY	=	83.025
THETA	=	.939

Figure 4.1-24. Image 291

```
................
................
.......++.......
......+++++.....
......++0++.....
.......+++......
................
................
................
```

Figure 4.1-25. Cuer-Output, Image 300

```
........
........
....11..
...11111
...11111
....111.
........
........
```

Figure 4.2-26. Tracker Reference, Image 300

show the tracker output for images 301 and 302; the circled 1's correspond to the circles in Figures 4.1-16 and 4.1-17 bounded by the symbol .
From Figures 4.1-16 and 4.1-17, we see that neither of these is at the appropriate target position. Further, in Figure 4.1-17, we see the target (2 small spots) emerging from the obscuration. To repeat in more detail, the reference tracker image for image 300 is shown in Figure 4.1-26 and the tracker output for image 300 is shown in Figure 4.1-27. At image 300, from Figure 4.1-26, the frame-to-frame tracker is solidly on the target. Referring to Figure 4.1-28, Image 301, we see that the dark spot is solidly covering the target. Since the bandpass correlation tracker, described in Section 2.0 of this report, is being used, it jumps to the upper left of the obscuration where it can find gray levels in the bandpass. This false target is shown circled on Figure 4.1-28. In Figure 4.1-29 image 302, the tracker then jumps to the bottom of the track window and grabs the circled false target. The real target is shown emerging to the left of the dark obscuration. So the binary correlation tracker has broken track; let us now consider several approaches to restoring track.

We discuss several approaches for restoring track in terms of images 287-292, Figures 4.1-2 through 4.1-17. This is the same, relatively simple, set we used to describe the interaction between cuer and frame-to-frame tracker. We shall then apply the track restoring approaches to images 300 and beyond where the obscuration occurs.

The geometry of the first series of images are shown in Figures 4.1-2 through 4.1-17, images 287 through 302. Image 287 is segmented for a best match on the target as shown in Figure 4.1-18. The histograms of the target, first sector ahead of the target, second sector ahead of the target, and the sector behind the target and the number of edge/perimeter match points on the target at less than or equal to the threshold are shown in Figure 4.1-30. Here it is seen that the target is moving into a darker background with no gray

		HISTOGRAMS			
Threshold	Target Matches	Target	First Sector Ahead of Target	Second Sector Ahead of Target	Sector Behind Target
14	10	12			
15	10	2			
16	17	8			
17	25	12			
18	25		3		2
19			6		3
20			8		16
21			5		20
22			10		11
23			14	4	
24			4	19	
25			4	25	

Figure 4.1-30. Matches and Histograms for Image 287.

```
................
................
................
................
................
................
........11......
.......11111....
.......11111....
........111.....
................
................
................
................
................
................
```

Figure 4.1-27. Tracker Output, Image 300

```
1111............
................
................
................
................
................
................
................
................
................
................
................
................
................
................
```

Figure 4.1-28. Tracker Output, Image 301

```
................
................
................
................
................
................
................
................
................
................
................
................
................
....111.........
....111.........
111111111.......
```

Figure 4.1-29. Tracker Output, Image 302

levels equal to those of the target. The background is segmented from the darkest level to the lightest for the change detection reference image; the threshold selected must be more than the target highest gray level to exclude the target from the background (Fig. 4.1-31). The direct segmentation of Figure 4.1-18, from low to high, is used to set the reference image for the tracker as shown in Figure 4.1-19 and the frame-to-frame track results are shown in Figures 4.1-20 through 4.1-24 for images 287 through 291. The change detection results of image 287 versus 292 are shown in Figure 4.1-32. The direct segmentation of image 292 is shown in Figure 4.1-33. Since there were no similar gray levels in the sectors ahead of the target in image 287, the direct segmentation is preferred and the blob found is used as the reference image for the tracker and image 292. This then describes a complete cycle and the interaction between the cuer, target signature prediction, change detector, and frame-to-frame tracker. With this in mind, we jump to image 300, Figure 4.1-15 and consider the remaining images.

For image 300, the cuer obtains a direct segmentation of the target APC as shown in Figure 4.1-34. The histograms of the target and surrounding sectors are shown in Figure 4.1-35. The sector ahead is seen as substantially darker than the target, hence, it is very possible that a direct segmentation of the target will produce maximum matches at a higher threshold than previously obtained. However, there are no gray levels ahead which are equal to those of the target which means that the target will remain segmentable unless it becomes obscured by the new background (e.g. passing into a woods). In any event the direct segmentation of the target in image 300 produces the reference track window shown in Figure 4.1-27. From images 301 and 302, due to obstruction of the target by the burn spot, Figures 4.1-28, 29, the frame-to-frame tracker has broken lock. A direct segmentation of image 303 (Fig. 4.1-36) shows the target about where expected and at a darker gray level, also, as expected. So even though the frame-to-frame tracker has lost the target, direct segmentation

CROSSING TARGET 2 THRESHOLD DOWN

P R O C E S S E D   C O L O R   A R R A Y

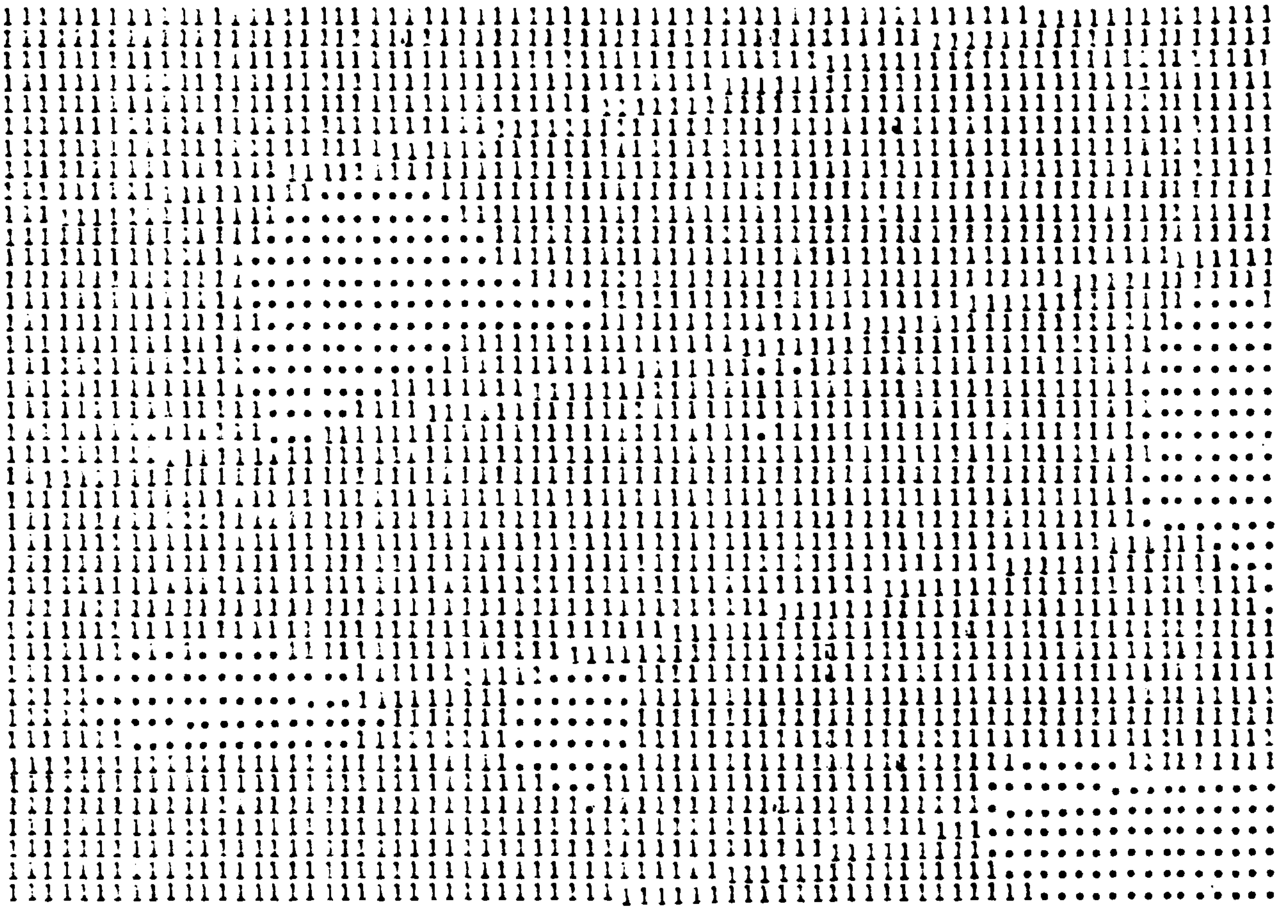

B L O B   S T A T I S T I C S

BLOB	AVG	TOPX	TOPY	BOTX	BOTY	XBAR	YBAR
1. 1	23.54	62	68	68	108	43.21	87.24

B L O B   I D E N T I F I C A T I O N S

	MATCHES
1. 1	333

Figure 4.1-31. Image 287

CROSSING TARGET - THRESHOLD DOWN

P R O C E S S E D   C O L O R   A R R A Y

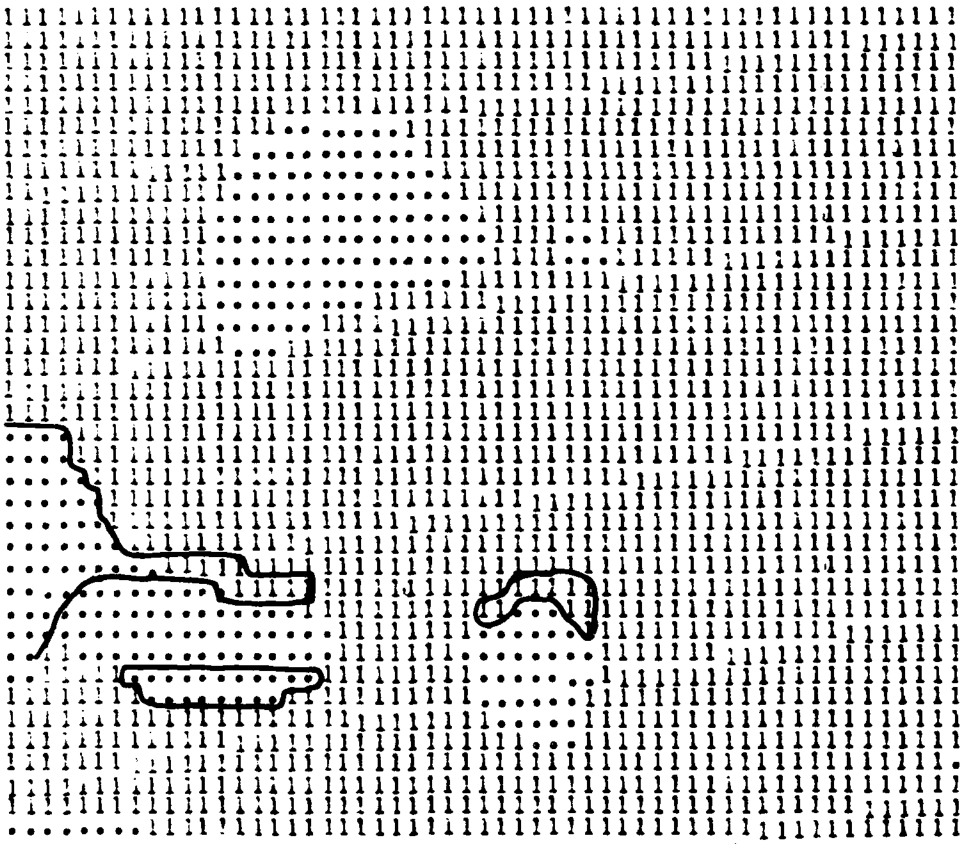

B L O B   S T A T I S T I C S

BLOB	AVG	TOPX	TOPY	BOTX	BOTY	XBAR	YBAR
1. 1	22.93	82	61	82	98	57.[illegible]3	79.22

B L O B   I D E N T I F I C A T I O N S

	MATCHES
1. 1	274

Figure 4.1-32. Image 292

CROSSING TARGET 2 THRESHOLD DOWN

P R O C E S S E D   C O L O R   A R R A Y

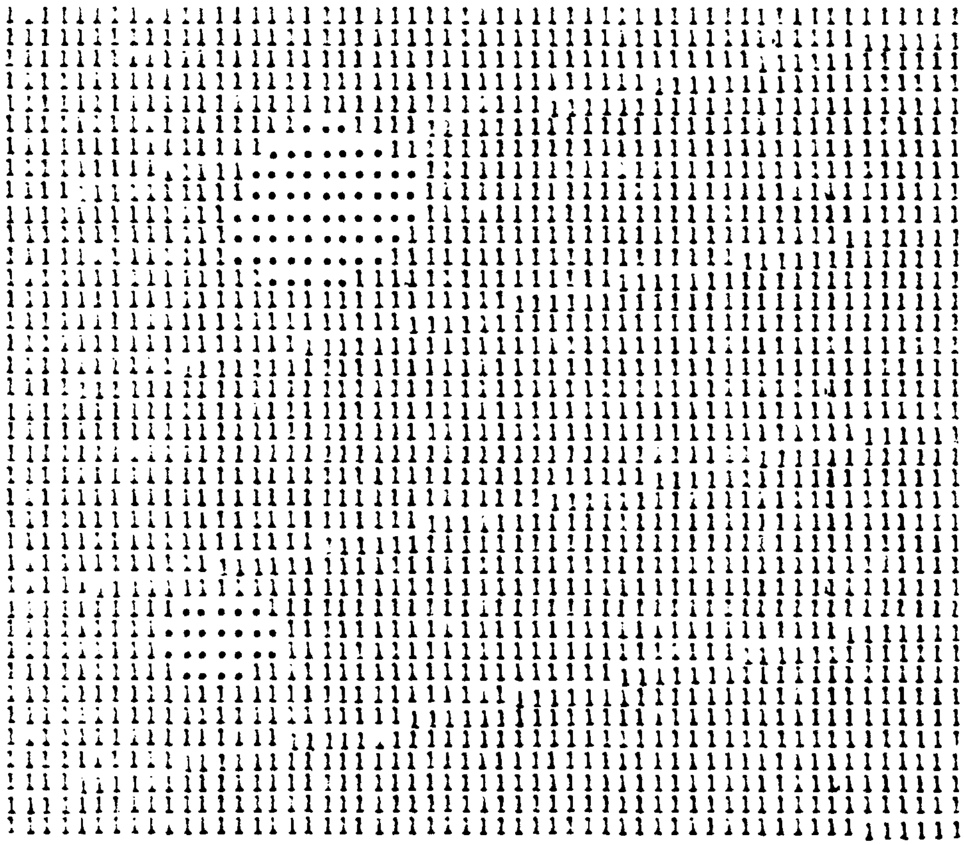

B L O B   S T A T I S T I C S

BLOB	AVG	TOPX	TOPY	BOTX	BOTY	XBAR	YBAR
1. 1	22.35	82	51	62	98	55.47	79.7[illegible]

B L O B   I D E N T I F I C A T I O N S

	MATCHES
1. 1	2[illegible]9

Figure 4.1-33. Image 292, Direct Segmentation

PROCESSING TARGET ? THRESHOLD DOWN

P O C E S S E D   C O L O R   A R R A Y

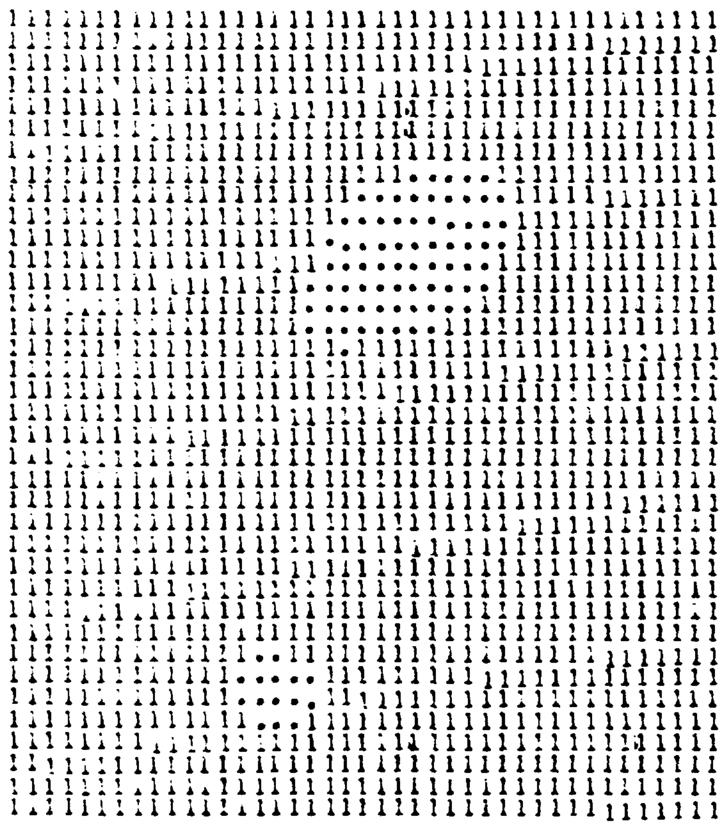

B L O B   S T A T I S T I C S

BLOB	AVG	TOPX	TOPY	BOTX	BOTY	XBAR	YBAR
1. 1	27.17	9[illegible]	50	9[illegible]	86	69.92	6[illegible].35

B L O B   I D E N T I F I C A T I O N S

	MATCHES
1. 1	17[illegible]

Figure 4.1-34. Image 300, Target

Threshold	Target Matches	Histogram Target	First Sector Ahead	Second Sector Ahead	Sector Behind Target
14	6	4			
15	14	2			
16	Max 18	9			
17	20	23			
18					6
19			4		6
20			1		6
21			1		
22			2		
23			0	2	
24			1	2	
25			1	3	
26			1	4	
27			1	6	
28			2	5	
29			2	2	
30			1	3	
31			2		
32			4		
33			4		

Figure 4.1-35. Histogram of Sectors and Target

DISAPPEARING TARGET 2 THRESHOLD DOWN

P R O C E S S E D   C O L O R   A R R A Y

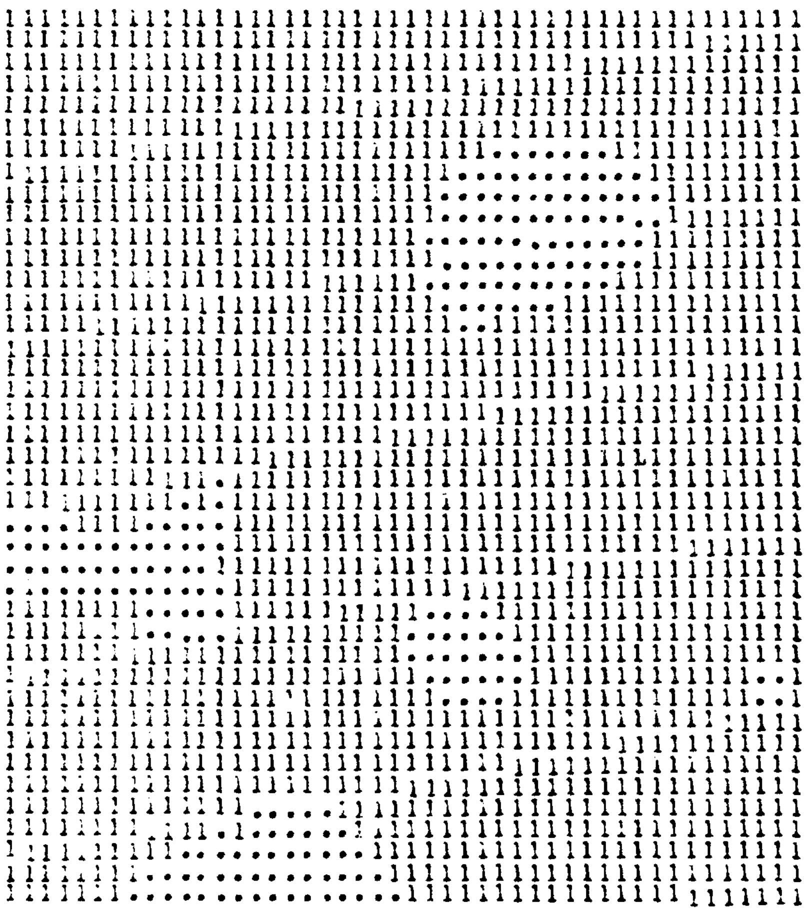

C O L O R   S T A T I S T I C S

COLOR	AVG	TOPX	TOPY	BOTX	BOTY	XBAR	YBAR
1. 1	27.86	82	26	92	66	69.77	45.62

Figure 4.1-36. Image 303, T $\leq$ 19

retains the target. Let us examine the change detection results to see if they are applicable in this case.

For change detection, we compare the background of image 303 thresholded at $t \geq 20$ with the background of image 300 thresholded at $t \geq 19$. Image 303 is shown in Figure 4.1-37 and image 300 is shown in Figure 4.1-38. The change detection results are superimposed on image 303, Figure 4.1-37. At first glance, the change record seems unintelligible. However, note that the change record in the lower, center part of Figure 4.1-37 has a dark and light portion; both portions are new. They are new in the sense that they did not appear in image 300. We are looking for a light target, and there is a light part of the change record in the anticipated target position. Hnece, knowing what to look for (approximate target location, polarity) in the change record is a significant advantage. Figure 4.1-36 shows a direct segmentation on the target for image 303 and confirms the change record.

DISAPPEARING TARGET 2 THRESHOLD DOWN

P R O C E S S E D   C O L O R   A R R A Y

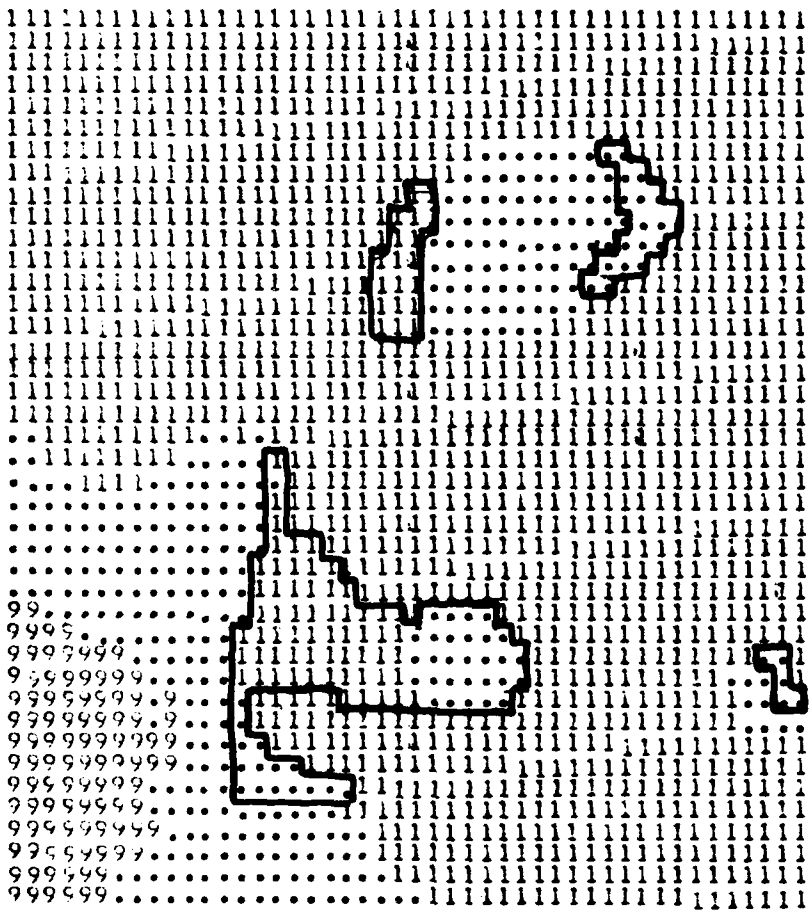

B L O B   S T A T I S T I C S

BLOB		AVG	TOPX	TOPY	BOTX	BOTY	XBAR	YBAR
1.	1	23.46	92	26	92	66	72.13	43.78
2.	9	2[illegible].25	48	[illegible]3	52	66	50.56	5[illegible].89

Figure 4.1-37. Image 303

CROSSING TARGET 2 THRESHOLD DOWN

P R O C E S S E D   C O L O R   A R R A Y

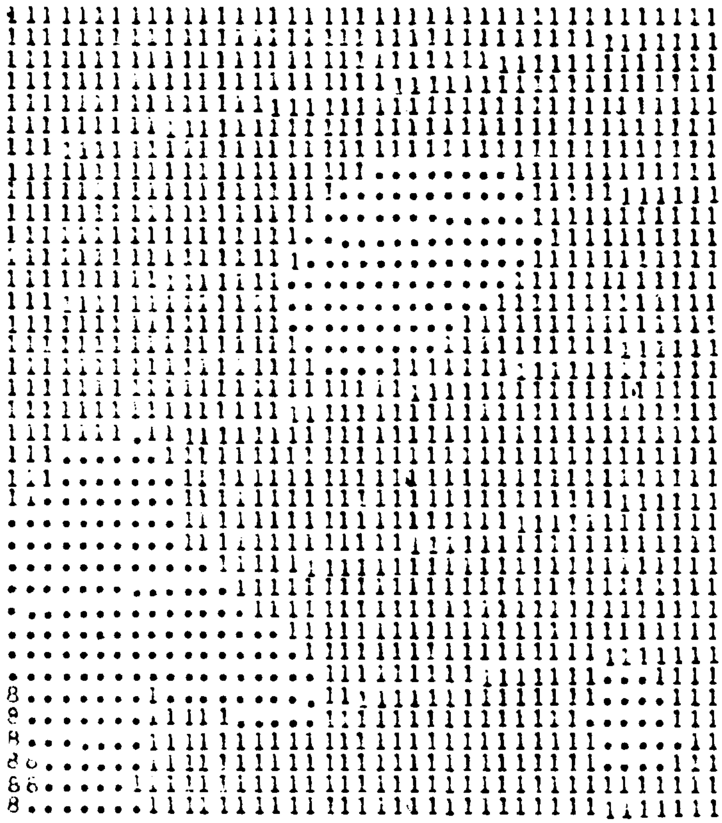

B L O B   S T A T I S T I C S

BLOB		AVG	TOPX	TOPY	BOTX	BOTY	XBAR	YBAR
1.	1	23.53	[illegible]	[illegible]	93	86	71.72	66.71
2.	8	19.[illegible]	57	81	50	86	50.25	83.75

B L O B   I D E N T I F I C A T I O N S

		MATCHES
1.	1	215
2.	8	5

Figure 4.1-38. Image 300

4.2 ROAD CROSSING CASE

In this example, an APC is moving onto a road from a field, as shown in Figure 4.2-1. The gray levels across the APC are in the range 10-14 while it is in the field. The road is at gray scale 0, and the surrounding field is in

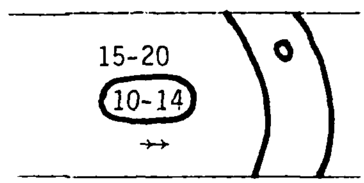

Figure 4.2-1. Road Crossing

the 15-20 range. As long as the APC is in the field, the target segmentation is clean as shown in Figure 4.2-2 for a threshold of 12. The statistics for each

```
.........................++
..........................0++
............................+
............................++
...............++0...........++          ← Left Edge
............+0000++...........+             of Road
............+0000++...........+
............+++++.............++
...............................+
..............................++
..............................+
```

Figure 4.2-2. Road Crossing, Edge-Perimeter Match (+), $t \leq 12$
(Image 290)

blob are shown in Figure 4.2-3. Blob number 2 is the target and blob number 1 is the road. For Blob number 1, the average gray level is 2.63; the x, y coordinates at the top are 81,23; the x, y coordinates at the bottom are 80,43; and the xy position of the centroid is 76.03, 32.43. This set of statistics gives no indication of any impending interference with the target, other than the fact that the target will intersect with the road because $BOTY_2 < BOTY_1$, and $TOPY_2 > TCP_1$. However, if we band threshold the image, i.e. find the gray scale

PROCESSED COLOR ARRAY

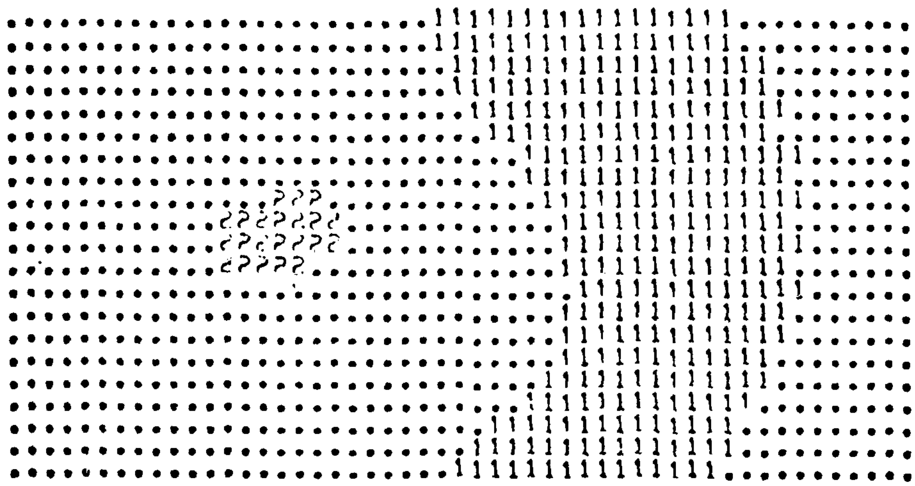

BLOB STATISTICS

BLOB		AVG	TOPX	TOPY	BOTX	BOTY	XBAR	YBAR
1.	1	2.63	81	23	80	43	76.03	32.43
2.	2	11.09	58	31	57	34	55.91	32.64

BLOB IDENTIFICATIONS

		MATCHES
1.	1	75
2.	2	14

Figure 4.2-3. Blob or Segment Statistics (Image 290)

range of the segmented target and then threshold the image at that band, we find a source of obscuration as shown in Figure 4.2-4. Here, blobs numbers 1 and 2 representing the shoulders of the road are also shown in Figure 4.2-4. This figure indicates that a clean, compact target segmentation cannot be obtained when the target is on the shoulder, and the classification logic will be defeated. Further, there is the possibility that the frame-to-frame tracker will "hang-up" on the shoulder. The band threshold has several drawbacks in that it is not backed-up by an edge coincidence and the band is not constant. That is, the gray scale of the target will fluctuate as seen in figures 4.2-5

```
P R O C E S S E D     C O L O R     A R R A Y

............................111.............222....
............................111..............222...
............................1111.............22....
.............................1111.............22...
.............................11111............22...
..............................11111...........222..
...................333........11111...........222..
...............33333333........11111...........222.
..............333333333.........1111...........22..
.............33333333333.........1111..........222.
.............3333333333...........111..........22..
...............333333.............111..........222.
...................................11.........222..
...................................11.........222..
..................................111........22....
...................................11........22....
..................................11........22.....
..................................11........222....
................................1111.......222.....
............................1111111........22......
........................11111111.........222.......
.....................1111111111.........222........
```

B L O B   S T A T I S T I C S

BLOB		AVG	TOPX	TOPY	BOTX	BOTY	XBAR	YBAR
1.	1	9.12	106	56	105	77	107.33	67.30
2.	2	8.51	122	56	118	77	121.79	66.56
3.	3	12.26	97	62	96	67	94.04	64.74

B L O B   I D E N T I F I C A T I O N S

		MATCHES
1.	1	15
2.	2	12
3.	3	7

Figure 4.2-4. Image Threshold at Gray Level Band of Target.

through Figure 4.2-10. A constant band of 10-14 would have caused holes in the target for images 310, 410, and 470. The lack of clean, compact segmentation is seen in Figure 4.2-10. More specifically, the cuer cannot give the frame-to-frame tracker a clean image for a reference. At this point, we have described two problems: 1) predicting obscuration, and 2) segmenting in the presence of obscuration. Further, can we estimate the distance between the target and the impending obscuration?

Target Road

18	18	17	17	17	17	16	16	16	17	17	17	17	17	17	16	15	13	13	13	11	08	03	01	0	0	0
17	17	17	16	16	14	14	14	15	16	16	17	17	17	16	16	15	13	13	13	11	09	05	01	0	0	0
17	16	16	13	13	11	11	12	14	14	15	16	17	17	17	17	16	15	15	15	13	11	09	05	0	0	0
16	13	12	11	10	10	10	11	12	14	16	17	17	17	17	17	17	16	16	16	16	13	09	05	0	0	0
16	13	12	11	10	10	10	11	12	14	17	18	18	18	18	18	18	18	18	16	16	16	10	05	02	0	0
16	13	12	12	11	11	12	16	19	20	20	20	20	19	19	19	19	19	19	17	17	16	10	05	01	0	0
18	18	18	18	18	19	20	21	21	22	22	22	22	22	21	20	19	19	19	19	19	16	13	07	03	01	0

Figure 4.2-5. Image 290, Target and Road

Target Road

19	19	18	18	17	17	17	16	16	16	15	16	16	16	17	16	16	16	15	11	10	07	05	03	01	0	0	0
19	18	17	16	16	16	15	15	14	14	14	15	15	15	16	16	16	16	15	13	11	10	07	09	02	0	0	0
18	17	16	15	13	12	11	11	12	13	13	14	15	15	16	16	16	16	15	15	13	12	10	07	04	01	0	0
17	16	15	12	12	12	11	11	12	12	13	14	15	15	16	16	16	16	16	15	15	13	10	07	09	02	0	0
17	16	14	12	12	11	11	11	11	11	12	13	14	15	16	17	17	17	17	16	16	15	14	10	07	04	0	0
17	17	14	12	12	11	11	11	11	11	12	14	15	16	17	18	18	18	17	17	17	16	15	12	08	04	0	0
18	17	15	15	12	12	12	12	13	14	15	16	17	18	18	18	19	18	18	18	17	17	15	14	12	06	01	0
20	19	18	17	16	17	17	17	17	19	20	21	21	21	22	22	22	20	20	19	18	17	17	15	11	04	01	0

Figure 4.2-6. Image 300, Target and Road

Target Road

18	17	17	16	16	16	16	16	16	16	16	16	16	16	16	15	15	15	11	09	04	0	0	0	0	0	0
17	17	17	16	15	14	13	13	14	15	16	16	16	16	16	16	16	15	14	10	08	02	0	0	0	0	0
17	16	16	14	13	11	09	09	12	12	15	16	16	16	16	16	16	16	15	12	09	04	02	0	0	0	0
16	14	13	11	08	08	08	08	09	10	15	15	16	16	16	17	16	16	16	13	11	08	04	02	0	0	0
16	14	13	11	08	08	08	08	09	10	15	16	16	17	17	17	17	17	16	16	12	09	06	13	01	0	0
16	16	15	14	10	09	09	09	12	15	16	16	18	18	18	18	18	17	17	16	13	11	08	05	03	0	0
16	16	16	16	18	19	20	21	22	22	23	23	24	24	24	23	22	19	18	16	19	12	06	05	03	0	0

Figure 4.2-7. Image 310, Target and Road

18	18	17	16	15	15	15	15	15	16	17	17	17	17	16	15	14	12	08	04	03	0	0	0	0	0
18	16	14	13	13	11	11	11	13	13	13	16	16	17	16	16	15	14	13	11	11	07	03	0	0	0
16	14	13	11	08	08	08	09	09	13	17	17	17	17	17	16	16	14	12	08	07	03	01	0	0	0
16	14	13	11	08	08	08	09	09	13	17	17	17	17	17	17	17	17	16	16	15	13	07	01	0	0
15	14	13	11	08	08	09	16	18	19	20	20	20	21	20	20	19	19	15	12	07	07	03	0	0	0
16	16	16	16	18	18	19	20	21	22	22	22	22	22	22	22	22	20	19	18	16	14	07	03	0	0

Figure 4.2-8. Image 410, Target and Road

18	18	18	18	18	18	17	17	17	16	16	15	15	14	12	08	02	0	0	0	0	0	0	0
17	17	16	16	16	16	13	12	12	15	15	15	15	15	15	13	05	01	0	0	0	0	0	0
17	16	15	15	12	10	09	09	10	11	13	15	15	15	14	12	09	02	01	0	0	0	0	0
16	15	14	13	12	10	09	09	10	11	13	15	15	15	15	14	10	05	01	0	0	0	0	0
15	13	12	12	12	12	10	10	11	15	15	16	17	18	17	15	12	06	04	01	0	0	0	0
15	13	12	12	12	13	14	15	15	16	18	19	20	20	20	17	14	10	05	03	01	0	0	0
18	17	14	14	14	15	16	16	19	21	21	22	22	22	22	20	19	14	09	05	03	01	0	0
18	20	22	23	23	23	23	23	23	23	23	23	23	23	22	20	19	14	09	06	04	01	0	0

Figure 4.2-9. Image 470, Target and Road

17	18	17	17	17	17	17	17	16	15	14	13	09	06	04	02	0	0	0	0	0	0	0	0
17	17	17	17	17	15	14	14	14	14	13	12	10	09	06	04	02	0	0	0	0	0	0	0
17	16	15	14	13	12	12	12	12	12	13	12	12	10	09	06	04	02	0	0	0	0	0	0
16	13	13	11	11	10	10	10	10	10	11	12	12	12	10	09	06	05	02	0	0	0	0	0
16	13	13	11	11	10	10	10	10	10	11	12	12	12	12	12	10	06	03	0	0	0	0	0
16	16	14	12	12	11	11	11	12	12	14	14	14	14	14	13	12	10	06	03	0	0	0	0
16	16	14	13	12	12	13	15	15	15	16	17	19	18	19	16	14	12	09	04	0	0	0	0
18	17	18	18	20	20	21	22	22	22	23	23	23	20	19	19	17	15	12	08	02	0	0	0

Figure 4.2-10. Image 480, Target and Road

The band threshold approach gives only an approximate measure of the distance between the target and the obscuration. Referring to Figures 4.2-11 thru 4.2-15 representing images 300, 310, 410, 470, and 480 the measured and calculated distances are shown in Table 1.

PROCESSED COLOR ARRAY

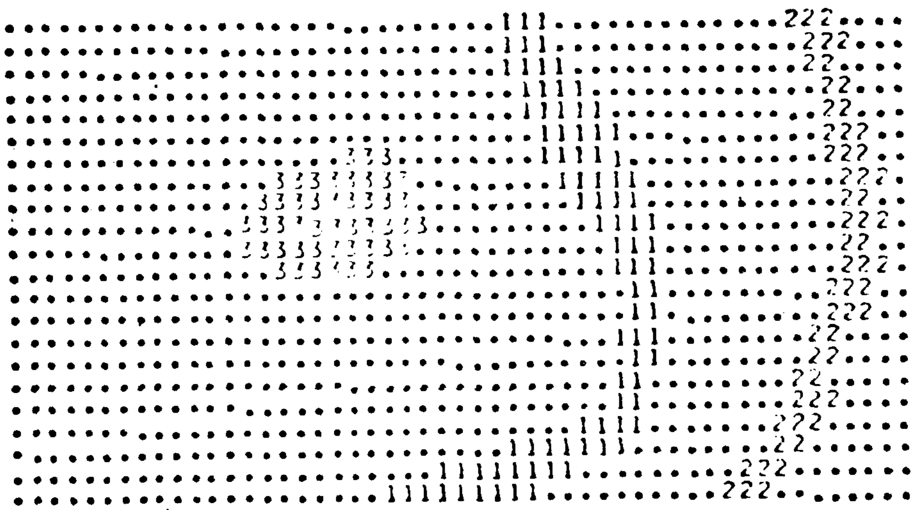

PLOT STATISTICS

	PLOT	AVG	TOPX	TOPY	BOTX	BOTY	XBAR	YBAR
1.	1	9.12	100	56	105	77	107.33	67.30
2.	2	7.51	122	56	118	77	121.79	66.56
3.	3	12.26	97	62	96	67	94.04	64.74

Figure 4.2-11. Image 300, Banded with Statistics

```
P R O C E S S E D     C O L O R     A R R A Y

.....................1111...........222222
.....................1111............22222
.....................11111............2222
......................11111.............22
........................111..............2
........................1111.............2
..........................111.............
.............3333.........111.............
...........3333333.........111............
.........33333333..........1111...........
.........33333333...........1111..........
...........333333...........11111.........
............................11111.........
............................11111.........
............................1111..........
............................1111.........6
...........................1111.........66
...........................111.........666
..........................11..........666.
........................1111.........66...
.....................11111..........66....
```

B L O B   S T A T I S T I C S

	BLOB	AVG	TOPX	TOPY	BOTX	BOTY	XBAR	YBAR
1.	1	8.42	109	86	110	106	111.80	95.92
2.	2	8.11	126	86	126	91	124.32	87.47
3.	3	10.71	101	93	101	97	98.46	95.17
4.	6	8.08	126	101	122	106	124.00	103.59

Figure 4.2-12. Image 310, Banded with Statistics

```
....................11111............222......
....................1111.............22.......
.....................11111............22......
.....................1111............22.......
......................11111............44.....
......................11111...........44......
........66666666.......111111...........77....
.......666666666.......11111...........9......
.......666666666...........11...........ØØØ...
.......666666............1111..........2......
...........................111..........6̸6̸....
.........................1111..........6̸6̸.....
...........................111.........6̸6̸.....
.........................1111.........76̸......
.........................1111.........76̸......
........................1111........76̸6̸.......
........................111.........76̸6̸.......
......................1111.........6̸6̸6̸........
......................11...........6̸6̸6̸........
....................111...........6̸6̸6̸.........
...................1111..........6̸6̸6̸..........
```

BLOB STATISTICS

Blob		Avg.	TOPX	TOPY	BOTX	BOTY	XBAR	YBAR
1.	1	8.52	27	21	25	42	27.42	30.17
2.	2	8.88	42	21	41	24	40.89	22.33
3.	4	8.25	43	25	42	26	42.00	25.00
4.	6	10.87	18	27	15	30	13.84	28.41
5.	7	9.80	44	27	44	27	43.90	27.80
6.	9	4.00	42	28	42	28	42.00	28.00
7.	Ø	8.67	49	29	45	29	44.00	29.00
8.	7	4.00	42	30	42	30	42.00	40.00
9.	6̸	8.14	44	31	38	41	40.07	36.54

Figure 4.2-13. Image 410, Banded with Statistics

```
..................1111.............222.......
..................1111..............22.......
...................1111..............22......
....................111..............22......
....................111...............2......
.............333.....111..............2......
...........3333333...111..............2......
.........333333333....111.............2......
........33333333.......111............2......
........333333.........1111..........22......
.........333............1111.........22......
........................1111........222......
.........................1111.......222......
........................1111.......222.......
```

BLOB STATISTICS

Blob		Avg	TOPX	TOPY	BOTX	BOTY	XBAR	YBAR
1.	1	9.10	63	52	59	72	63.77	62.32
2.	2	7.94	79	52	74	72	77.60	63.36
3.	3	11.72	57	57	53	62	54.28	59.44

Figure 4.2-14. Image 470, Banded with Statistics

```
 ................1111...............2.......
.................1111...............2.......
..................1111..............22......
..................11111..............2......
..............1111111111.............22.....
...........11111111111111............22.....
.........11111111111111111............22....
.........111111111111111111..........222....
..........111111111111111111..........22....
..........11111.........1111.........22.....
..........................11.........222....
..........................11........222.....
..........................111.......222.....
.........................111.......222......
```

BLOB STATISTICS

Blob		Avg.	TOPX	TOPY	BOTX	BOTY	XBAR	YBAR
1.	1	10.23	97	78	79	107	92.01	91.78
2.	2	7.67	113	78	112	96	113.80	87.77

Figure 4.2-15. Image 480. Banded with Statistics

Table 4.2-1. Distance to Obscuration

IMAGE	XBAR TARGET	XBAR OBSCURATION	CALCULATED DXBAR	DISTANCE (MEASURED)
300	94.04	107.33	13.29	9
310	98.46	111.80	13.24	9
410	13.84	27.42	13.58	7
470	54.28	63.77	9.49	3
480	92.01	92.01	0	2

We compute a probable intersection of objects 3 and 1 by noting that $TOPY_1 < TOPY_3$ and $BOTY_1 > BOTY_3$. Figures 4.2-12, 4.2-13, and 4.2-14 show the bands for images 310, 410, and 470. These images show that an (intersection) obscuration is imminent. However, the XBAR statistic does not give a true indication of the "distance to obscuration." For example, Table 4.2-1 shows the distance to obscuration in terms of XBAR and actual distance. The actual distance is measured by counting the pixels between the right edge of the road target and left edge of the road border. The precise number of pixels to obscuration may or may not be needed. This depends to some extent on hardware implementation. It is enough to know at this point that the prediction of obscuration may be off in the distance by the centroid approach by 60 percent of the target width. In Figure 4.2-15, image 480, we see the case where obscuration of the target front end has occurred.

Another approach to the obscuration prediction and distance to obscuration problem is the use of histograms to detect regions ahead of the target which have the same gray levels as the target. In image 470, Figure 4.2-9, histograms one and two target widths (mutually exclusive) in front of the target and one target height are shown in Figure 4.2-16 as well as a histogram of the target. Figure 4.2-16 shows that the background one target width in front of the target will have gray levels the same as the target. However, for two target widths in front, the background will be different again. It is also different from the

background one target width in front. Both the band threshold and histogram approaches predict obscurations which fall in the same gray scale range as that of the target. We now address segmentation in this region.

GRAY LEVEL	ONE TARGET WIDTH (F)	TWO TARGET WIDTHS (F)	TARGET	ONE TARGET WIDTH (B)
20	3			
19	1			3
18	0			8
17	3			7
16	2			5
15	10			6
14	3			1
13	1		6	
12	2		10	
11	0		3	
10	3		6	
09	1		4	
08		1		
07		2		
06		1		
05	1	1		
04		1		
03		1		
02		1		
01		5		
00		28		

(F): Front
(B): Behind

Figure 4.2-16. Histograms of Background and Target; Image 470

Since a clean segmentation does not seem possible with the present segmentation algorithms we are faced with changing them or retaining enough of the target to maintain a coherent track. We shall try the latter. Heuristically consider what happens as the target approaches the road shoulder. The front of the target merges with the shoulder, while the rear is clearly visible against the darker background of the field. Further, as the target moves onto the road, the target gray scale becomes lighter as shown in Figure 4.2-17, image 590.

			Target										Road												
17	16	14	12	09	05	03	01	0	0	0	0	0	0	0	0	0	0	0	0		02	06	09	13	14
17	16	14	13	11	09	05	03	01	0	0	0	0	0	0	0	0	0	0	0	0	02	04	07	12	14
17	16	15	13	12	10	07	05	03	01	0	0	0	0	0	0	0	0	0	0	0	0	02	05	11	14
17	16	15	13	11	09	07	05	04	03	01	0	0	0	0	0	0	0	0	0	0	0	02	05	10	14
17	16	14	13	11	09	07	05	04	03	03	02	01	01	01	01	0	0	0	0	0	0	01	04	07	14
17	16	13	12	10	07	05	04	04	04	04	04	05	05	07	06	02	01	0	0	0	0	01	02	06	11
17	15	13	09	05	05	04	04	04	05	05	06	07	07	07	07	07	05	02	01	01	01	01	02	05	10
16	13	11	09	05	05	04	04	05	05	07	08	10	12	12	12	09	07	04	02	01	01	01	02	05	09
17	15	12	10	05	05	05	05	08	09	11	14	15	17	17	17	14	10	07	09	02	02	02	03	05	09
17	17	15	12	11	12	12	13	15	16	22	22	22	22	22	21	17	15	10	08	04	03	03	05	09	12
18	17	17	17	19	21	21	22	22	22	22	22	22	22	22	21	18	17	15	11	09	06	06	09	12	14

Figure 4.2-17. Image 590, Target and Road

This prevents using fixed thresholds across the transition. As the target moves further onto the road, the target rear merges with the shoulder and the front of the target becomes more apparent against the road. One possible approach is to sense the onset of the new background, actually two backgrounds in this case, and obtain a segmentation of the new background using edge coincidence. We recognize the fact that we shall lose the front of the target, but the rear is retained. Hence, the frame-to-frame tracker can be directed to it. Once the target emerges onto the road the frame-to-frame tracker will be directed to the front. This is shown in Figures 4.2-18 and 4.2-19.

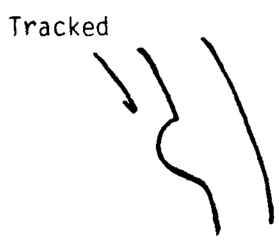

Figure 4.2-18. Direct Tracker to Rear of Target

Figure 4.2-19. Direct Tracker to Front of Target.

Since the target will appear on the road, as a dark target against a light background, we threshold down from the target and, obtain, as shown in Figure 4.2-20, the background. Registration and subtraction of Figure 4.2-20 with Figures 4.2-18 and 4.2-19 obtains the rear shape,  , and the front shape, , respectively. The tracker reference window is then offset so that this portion of the target is placed squarely in the center of the window. Consider now some aspects of the change detection process.

Figure 4.2-20. Background

A first approach is binary correlation using the Exclusive - OR function. The single biggest problem in these examples is the choice of thresholds for the binary correlation. We have discovered that the gray scale of the target changes as it moves from one background to the next; this means that trying to limit the thresholds, band them, or fix them ahead of time is not appropriate. Secondly, when we segment the background (the road in this case), the segmentation may include part of the road shoulder which has gray levels which merge with those of the target.

The histogram approach allows us to detect the obscuration regions (road shoulders) within the general background (road, in this case). Secondly, the histogram approach indicates the changing target/background polarities. For example, the histogram shows a gray target against a dark background for the target in the field. This histogram shows a gray target against a light background for the target on the road. The anticipated polarities define the threshold levels for binary change detection. For example, the threshold would be everything darker (above) than the target for the field background, and everything lighter (below) than the target for the road case. This approach assumes that the target outline against the road will produce strong enough

edges such that target outline is represented by a "hole" in the road. Having discussed the rationale and alluding to some of the problems we found in other approaches, we now move into the mechanics of the process.

The histogram of Figure 4.2-17 represents image 470 and is the last image obtained before the target moves on the road shoulder. Figure 4.2-21 shows the number of matches for various thresholds starting at low gray levels (light) and moving higher (darker). The maximum number of matches occurs at a threshold $\leq$ 12. The resulting image is shown in Figure 4.2-22a and 4.2-22b. The next image of concern is 480. The tabulation of matches is shown in Figure 4.2-23.

Threshold	Number of Matches	Number of Perimeter Points	% Matches
3	42	67	52
4	48	67	61
5	52	67	67
6	55	69	70
7	58	69	72
8	60	69	83
9	62	69	78
10	63	69	78
11	63		
12	65		

Figure 4.2-21. Tabulation of Matches, Image 470

```
.....................111111111111111111......
.....................111111111111111111......
..............22......11111111111111111......
...........222222.....11111111111111111......
...........222222......1111111111111111......
.........2222222.......1111111111111111......
.........222............111111111111111......
.........................11111111111111......
.........................11111111111111......
.........................11111111111111......
```

BLOB STATISTICS

BLOB	AVG.	TOPX	TOPY	BOTX	BOTY	XBAR	YEAR
I. 1	2.29	78	52	73	72	78.81	61.59
I. 1	10.87	57	57	53	61	54.71	59.12

BLOB IDENTIFICATIONS

	Matches
1. 1	65
2. 2	14

Figure 4.2-22a. Image 470 and Statistics

```
..............++0000000
...............+0000000
...............++000000
........++......+000000
.....++00++.....++00000
.....+000++......+00000
...00000++.......++0000
...+++............++000
...................+000
...................+000
```

Figure 4.2-22b. Image 470 and Matches

Threshold	Matches
6	102
7	104
8	111
9	113
10	116
11	119
12	137
13	134
14	137
15	136

Figure 4.2-23. Match Tabulation for Image 480

Then the change detected image is composed of image 470 thresholded at 12 and image 480 thresholded at 12. The resultant image is shown in Figure 4.2-24. The left portion of the remainder is positioned in the inner track window, which is just large enough to include 90 percent of the target.

The next change detection is done for images 470 and 590, i.e. we are trying now to capture the front of the target and place the frame to frame tracker there. Figure 4.2-25 is a tabulation of the matches for image 590. The appropriate threshold here is 10 and the change detection result is shown in Figure 4.2-26.

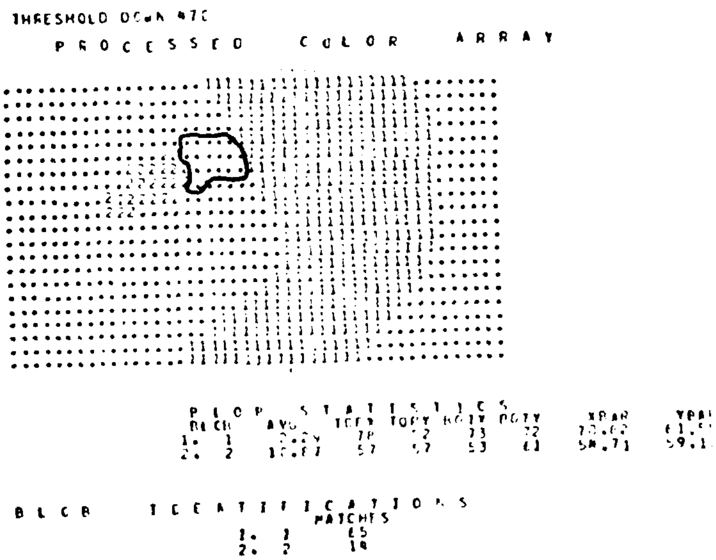

Figure 4.2-2[illegible]. Change Detection Result

Threshold	Matches
6	48
7	51
8	52
9	62
10	69
11	67
12	66
13	67
14	68

Figure 4.2-25. Match Tabulation for 590

In summary, we have described the mechanics of predicting an obscuration, estimating how the target signature will be affected, and moving the tracker to work around the obscuration.

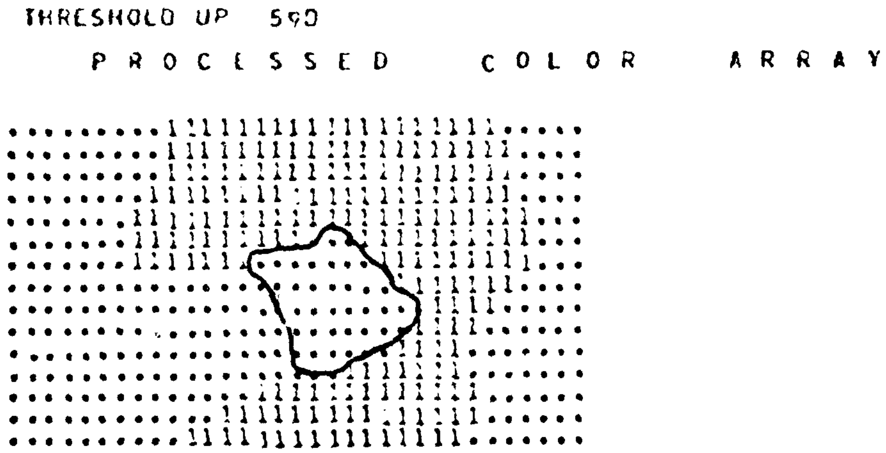

Figure 4.2-26. Change Detection Result

4.3 DISAPPEARING TARGET NO. 1

In this sequence, an APC is moving through a woods. The APC starts as a 7 line high target and becomes progressively smaller until it disappears among some trees. The range from the helicopter to the target appears to be closing. The purpose of analyzing this sequence is to discover those factors which can quantitatively anticipate and confirm a disappearance. Recognition of these factors will prevent the intelligent tracker from becoming "locked up" on a section of background which is left after the target is gone. Further, it allows the intelligent tracker to go into an reacquisition mode which is not the same as the acquisition mode. That is, since the approximate location of the target is known, change detection can be employed in this area which is less than the entire image, thus easing the hardware burden. It also means that it may be possible to reacquire the target, through change detection, without the need for seeing the entire target shape.

The sequence of images runs from 598 through 667. For images 598 through 638, every tenth image is segmented by the segmentation techniques described in Appendix A of the First Quarterly Report. From image 641 to completion, every fifth window is segmented with the exception of image 646 which was erroneously deleted during some computer file manipulations. Figures 4.3-1, 2, 3, 4, and 5 show the target in images 598, 608, 618, 628, and 638 as it disappears; the target is the blob on the left and the blob on the right corresponds to a small clearing in the woods. These images represent the raw gray scale divided by four and rounded to the nearest integer. This presentation allows the analyst to quickly see the more important features in an image. It is assumed that the intermediate frames (i.e. 599, 600, 601, 602, 603, 604, 605, 606, and 607 for the first interval) are processed by the binary correlation tracker. If the cuer does not detect the target disappearance, the binary tracker will continue to track whatever reference target is given to it. That is, if the cuer has transferred its

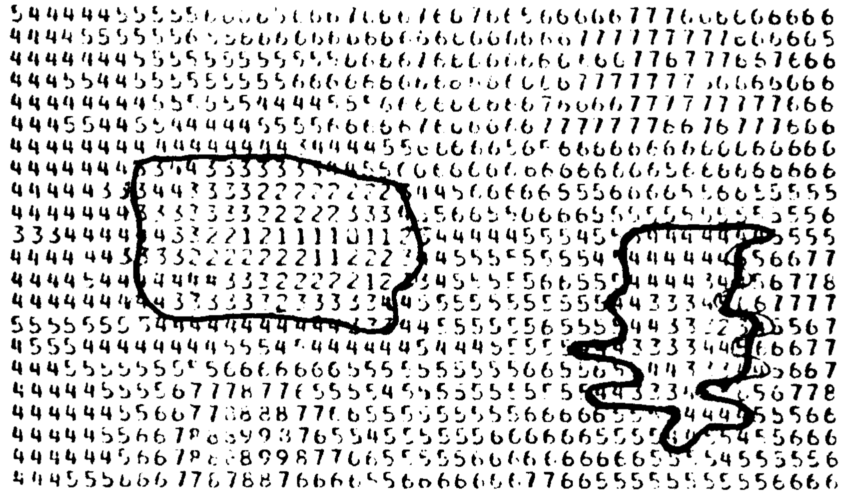

Figure 4.3-1. Image 598

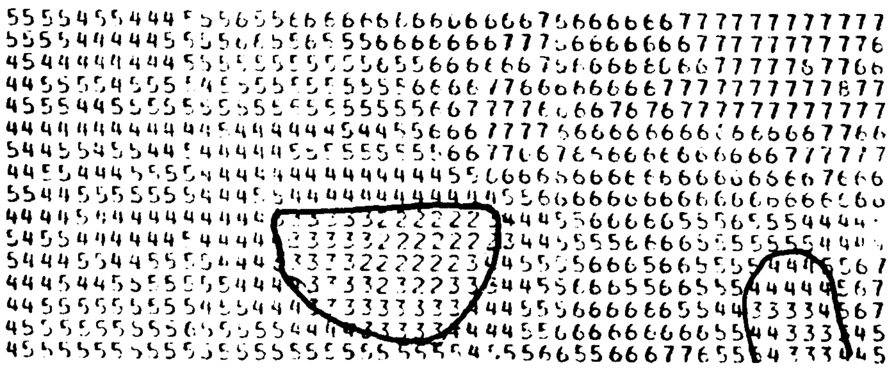

Figure 4.3-2. Image 608

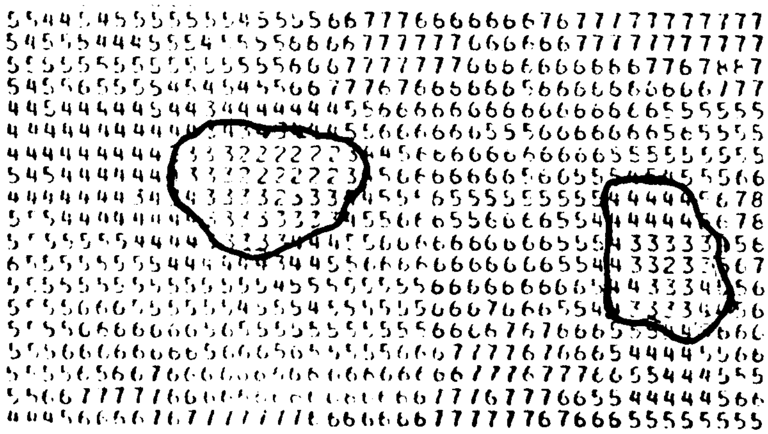

Figure 4.3-3. Image 618

```
5555545555555555555555666777888777777777777877778888
54555555555556555555566777777777777777777777778888
5444444555555555554555567778886777776677777777777777
555445555455555555555566777776766666666676677777
4444545555555555555555566677776666667677777776666
5544544454555555555555566666666666677676766555555
54445544544444443333333345566655555666666656555556
44445555544444433322222233445666666556666555555556
555455555544444443333333455666666656666666555555567
5555555544445544433444445666666666666666655444456678
55655555555544444444444445556656666666554433334567
5565555555554444343444455556666666665554433334466
556655566655555545555555555666666666665443333456
5555666666666666555556666556666666666665554444466
55555556666666655555665555566666667666655444445566
55556656667776666665666565556666667777676655555667
55555567777777767777666666667777777777766554555666
555555566677777777777777776676677777777776655555566
44445566777777777667766666677777777777776655555556
44444455667777777677777777767777788887777765555555
5444444566777777777777777766777888887776665665555
```

Figure 4.3-4. Image 628

```
55655555555556667888888877777777777777788888877777
5555554444555667788887777776777777777778888877
5555555554556677777777776666666777777777777777777
5555555545455556666666767666666666666555555555555
555555555555555666666666666666666666666666666666
4454445444444455555666666666666665555555555677777
54444444444334555667666656666666666555555566677777
44444444433333444455666665656565555555566677899
4444444444333345566666666666665555544444667889996
655445544455555555566666666666666555444444566788
5554444444454444555556666666666665554433334566788
65655555555555555555666666666666666554433344567887
65555555555555555566666677777766654444445677788
667666666665656666566667777776666665555566666777
6666666655555555555566666667777766554444455667777
66777776666666766666666777777777766555555666777
7887777766666666666666667777777777655555566666
7777767777777777777677777777777776666666665667
6677777777777666766777777777777766655555566666
5666777777877777767677777788888776665555555666
66766777777777776666677777777777666655555555566
```

Figure 4.3-5. Image 638

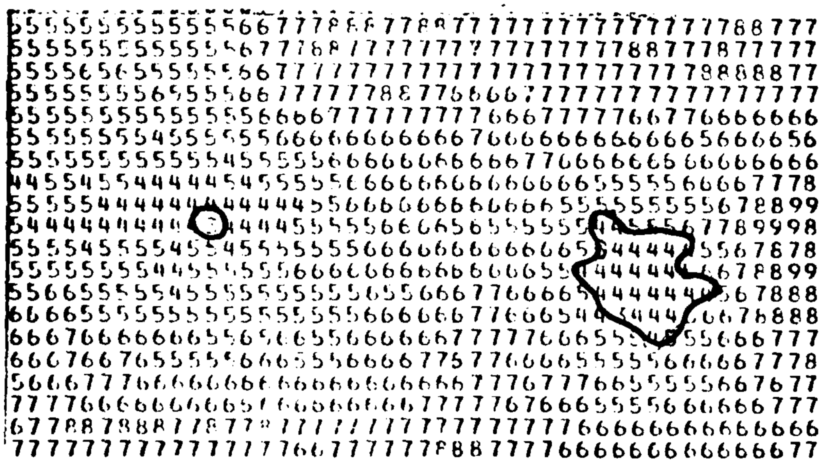

Figure 4.3-6. Image 641

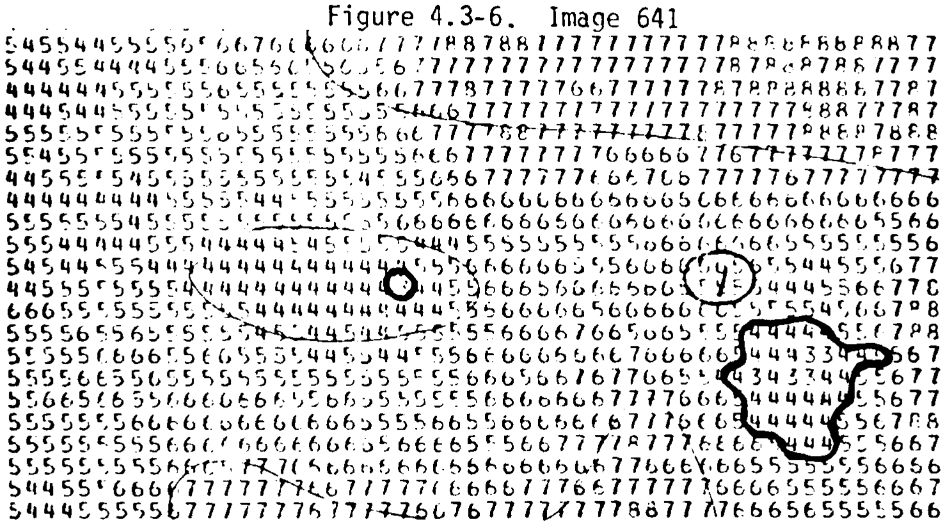

Figure 4.3-6a. Image 647

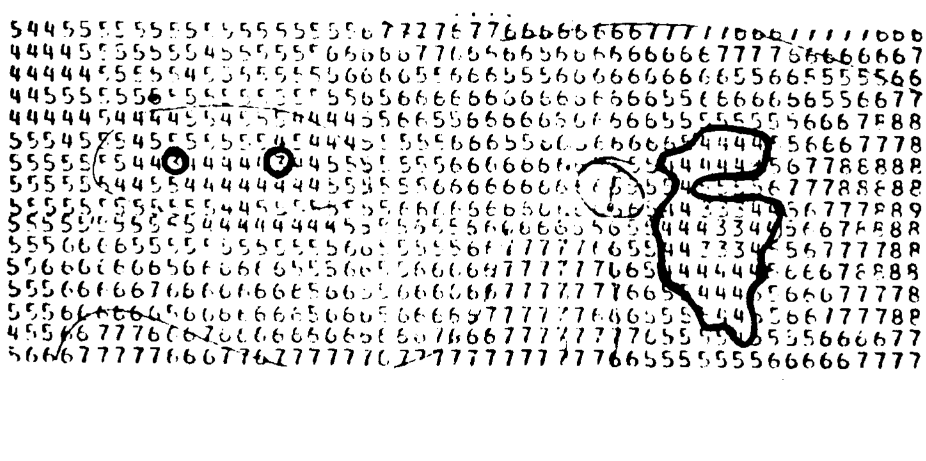

Figure 4.3-7. Image 652

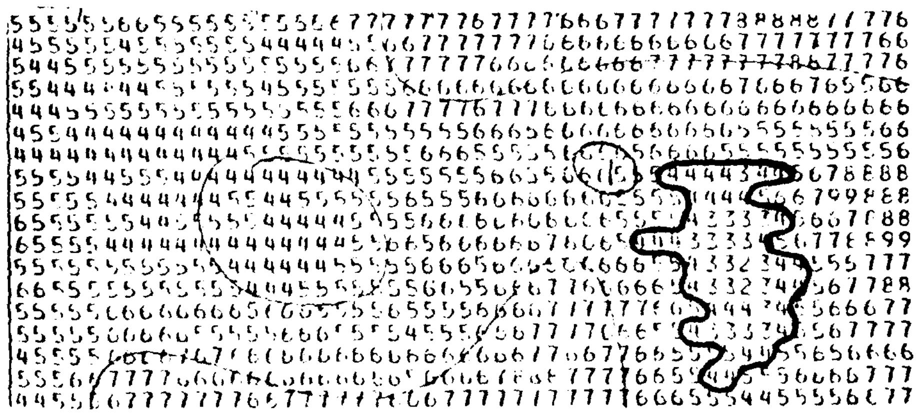

Figure 4.3-8. Image 657

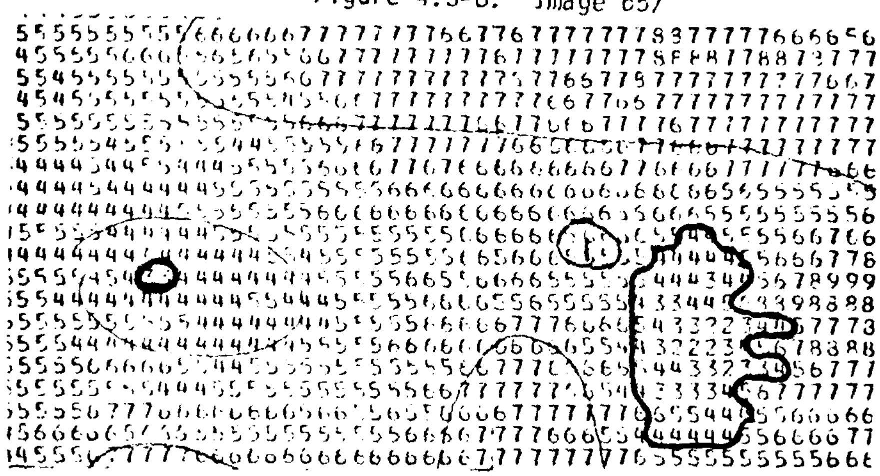

Figure 4.3-9. Image 662

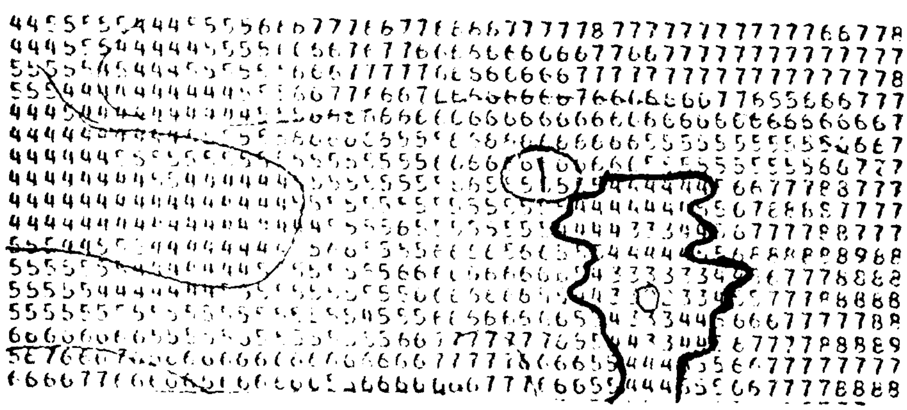

Figure 4.3-10. Image 667

attention from the target to the background, the binary tracker will track the appropriate portion of the background. The remainder of the cued images in this sequence are shown in Figures 4.3-6, ... 10. One might argue that the target is still present as seen in Figure 4.3-10, but the video tapes show the target disappearing in the same vicinity as already shown in Figure 4.3-6 (Image 241) and reappearing in another portion of the image. As can be seen in Figure 4.3-10, the target area has merged into that of the background. We have shown, in all these images, a clearing in the woods ahead of the point of disappearance which offers a source of trouble to a tracker which opens the track windows if and when it realizes that a loss had occurred. In this regard, several tracker experiments were conducted on this sequence which are described later in the Section (4.3). Consider now the problem of detecting a disappearance.

One might suggest that the intelligent tracker simply wait until the classification logic cannot classify the object and then move to a reacquisition mode. There are two reasons why this is probably not the best strategy. First, performance tests on existing cueing logic for classification indicates that there is room for improvement in both correct classifications and false alarm reduction. Second, in dense clutter such as exemplified by this sequence, the target may not reappear as unobscured. That is, it may reappear partially obscured. This condition implies an acquisition on a partially obscured target. To avoid this prospect, we can change detect on the background in the vicinity of the target disappearance to reacquire the target. The sensitive issue is the appropriate image of the background. If the target disappearance is not promptly detected and the target reappears as partially obscured but cannot be cued directly, it will be taken to be part of the background provided it does not move. On the other hand, a prompt detection of disappearance will allow the change detection algorithms to use a reference background in which the target has not reappeared thus allowing reacquisition of a reappearing, but partially obscured target. This case is considered in Section 4.6. Having discussed the rationale, let us consider the mechanics of detectiong a disappearance.

The idea of a background composed of homogeneous segments has been considered by several workers. Further, some of these efforts and others have been devoted to discriminating between targets and background on the basis of histogram properties which rely on homogenity properties. For example, the fourth moment of a histogram, kurtosis, denotes the peakedness of a histogram; the idea is that a histogram of a target would have a higher kurtosis than a histogram of the background (same window size) assuming the target is large enough to have an interim distribution of gray levels other than a uniform one. Clearly, a one-line high target does not, but a 7 or 8 line high target, from our experience, usually has some distribution. We compute the kurtosis for the target in image 638 and 641, Figure 4.3-5 and 4.3-6, respectively. The framework for the calculation is that kurtosis, α_4, is three for a normal distribution and $\sim$1.8 for a uniform distribution. Further the following table shows α_4 values for uniform distributions

Classes	Kurtosis
1	0
2	1
3	1.5
4	1.64
5	1.7
6	1.73
7	1.75
8	1.76

Figure 4.3-11. Kurtosis vs. Classes for a Uniform Distribution

with various numbers of classes. For image 638, there were four classes and the kurtosis was 1.04; in image 641, there were two classes and the kurtosis was 1.01. The expected result was a kurtosis approaching 3.0 for image 638. But in trying to apply the kurtosis criterion, we noticed another possible approach.

As we suggested earlier, a target seven lines high should have some gray level distribution. To this end, we computed the mean gray scale, GS, of the target and compared it with the superslice threshold, T. Further, we compared this against the background histogram in the first sector ahead of the target. The histogram computations were the histogram mode, that value occurring most often, and the "second mode", that value occurring the second most frequently. The results

are shown in Figure 4.3-12 and 4.3-13 for the images shown previously. In Figure 4.3-12, the histogram mode is circled and the second mode is enclosed in a square. The point of this figure is that in the vicinity of images 618 through 647, the background in front of the target is fairly constant.

IMAGE

Gray Level	598	608	618	628	638	641	647	652	657	662	667
16	1	0									
17	6	6									
18	1	0									
19	6	10	6							15	
20	9	3	3	5	8		2			16	
21	$\boxed{18}$	3	2	7	5	7	4	7	NO	14	NO
22	5	3	5	3	3	8	4	5	TARGET	6	TARGET
23	12	$\boxed{12}$	5	6	6	4	10	4		10	
24	19	32	37	22	$\boxed{20}$	$\boxed{15}$	$\boxed{12}$	8		1	
25			$\boxed{29}$	$\boxed{16}$	25	31	24				
26				5	8		6				
27							1				

Figure 4.3-12. Modes of Background Histogram

IMAGE

	598	608	618	628	638	641	647	652	657	662	667
$\overline{GS}$	12.1	13.72	15.95	16.73	18.	18.59	18.96	19	NT	18	NT
T	15	16	18	19	19	19	19	19		18	

Figure 4.3-13. Threshold vs. Average Target Gray Scale

In Figure 4.3-13, the superslice threshold is increasing which could be explained by the background histogram becoming darker. The average gray scale in the interior of the target is shown to be 12.1 for image 598; this means that the target has a light interior and, more importantly, a gray level

distribution across the target since $\overline{GS} < T$. However, $\overline{GS}$ begins to approach T which means that the target is becoming the same gray level throughout, while the background in front of the target is relatively constant. This condition is reinforced at image 657 in which no target blob can be segmented. Recall, on the video tape, the target is disappearing into a dense clump of trees; the dense trees can be characterized by the constancy of the histogram in front of the target. As the target disappears, the remaining target portions are enlarged as the segmentor picks up more and more of the background.

Another approach to the same problem produces the same result but perhaps a little more dramatically. The superslice algorithm for the case of a light target in a dark background slices up from zero. At each threshold, it forms a slice through the target so a succession of slices produces a set of laminations of increasing area. Normally, the process stops when a maximum number of matches is reached. We have been working with the idea of stopping sooner and tracking a bright interior portion of the target. For the sequence under discussion suppose the slicing is stopped, for purposes of tracking, (not identification), at a match of 70 percent, (i.e. when 70 percent of the perimeter points are matched with corresponding edges). In Figure 4.3-14, we show the slice threshold at which 70 percent of the matches occurred. The decided shift into higher thresholds is seen. The numbers in parenthesis are the target areas at each threshold. Thus, the light interior is vanishing while the target interior suddenly jumps in size and decreases in intensity, again signifying that the bright target interior has vanished. This is another indication that the target has disappeared in total.

As a side issue, the 70 percent figure was a byproduct of the work on a smaller gradient operator window described in the Second Quarterly. It appears, based on a limited number of samples, that the 70 percent figure ensures that a blob has a fair representation of edges for each of the four sides.

IMAGE

Threshold	598	608	618	628	638	641
11						
12	(36)71%	57%				
13		(25)83%				
14			(37)72%		(SIZE)	
15						
16				(24)70%	(6)83%	
17						
18						
19						(59)84%

Figure 4.3-14. 70% Thresholds and Target Area

In this section, we have described two lines of analysis for determining the disappearance of a target, (i.e., loss of interior highlights above super-slice thresholds, and loss of area of small bright interior details), there is nothing to preclude using both of them in a complementary fashion. In addition to this work on the sequence, we performed several small tracking experiments on it.

In the first tracking experiment, we looked at image 598 which had a target histogram ranging over 9-12; we set the band pass binary correlation tracker at 9-16 using only image 598 as a reference image. The tracker lost the target at image 614. Secondly, we used every other image to simulate the case where the tracker was multiplexed between two targets. Several things occurred: (1) the target moved out of the bandpass, and (2) the 8x8 inner window was too small to handle the larger target movements. When the cuer identified the target on frames 598, 608, 618, 628, and 638 and updated the band-pass of the tracker, track was maintained throughout. However, the binary tracker showed a tendency to slip to the rear of the target (Figures 4.3-15, ...20)

indicating that the inner track window was too small. It should be pointed out that the binary tracker was again given only every other window to track and track was not broken with every tenth image referenced for it by the cuer. The conclusion is that a bandpass binary correlation tracker has limited capability in a highly cluttered background. Continuous tracking is possible with a relatively simple tracker being updated by a cuer, and in this situation it is possible to share a tracker between two targets.

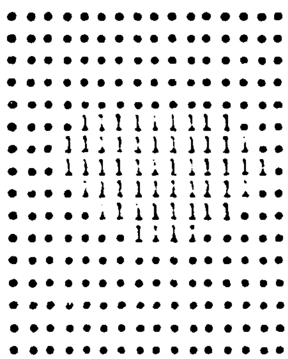

XBAR = 9.315
YBAR = 8.167
SIG2X = 95.819
SIG2Y = 68.981
SIGXY = 76.370
THETA = .670

Figure 4.3-15. Reference Image 608

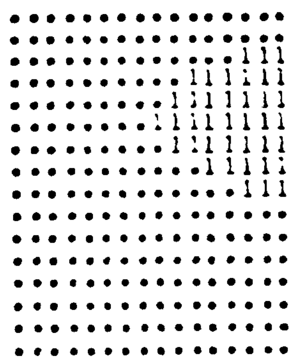

XBAR = 13.410
YBAR = 5.949
SIG2X = 183.821
SIG2Y = 78.256
SIGXY = 79.897
THETA = 1.155

Figure 4.3-16. Image 610

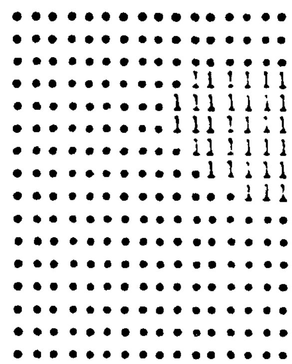

XBAR = 13.520
YBAR = 6.178
SIG2X = 185.618
SIG2Y = 48.998
SIGXY = 24.324
THETA = 1.141

Figure 4.3-17. Image 612

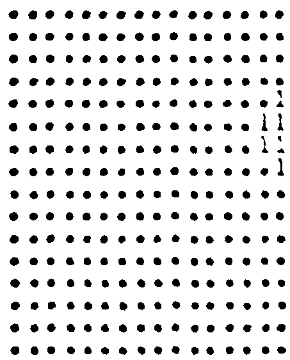

XBAR	=	15.667
YBAR	=	6.580
SIG2X	=	245.667
SIG2Y	=	43.167
SIGXY	=	101.633
THETA	=	1.177

Figure 4.3-18. Image 614

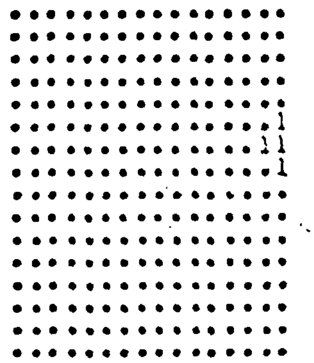

XBAR	=	15.750
YBAR	=	7.880
SIG2X	=	248.250
SIG2Y	=	49.800
SIGXY	=	118.250
THETA	=	1.152

Figure 4.3-19. Image 616

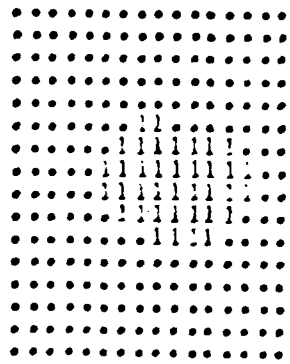

XBAR	=	9.974
YBAR	=	8.632
SIG2X	=	184.395
SIG2Y	=	76.421
SIGXY	=	86.431
THETA	=	.856

Figure 4.3-20. Image 618, Reference Image

In summary, we were not able to use the kurtosis computation to detect a target disappearance. The modes of a histogram of the background did not seem to add much insight to the problem. A more useful computation is the comparison of the Superslice threshold obtained through a maximum number of edge-perimeter point matches with the average gray scale over the target. The average gray scale approached the Superslice threshold even before the target disappeared as measured by the Smart Sensor segmentation processes.

4.4 CROSSING TARGET NO. 2

This is a second example of a dark target (simulated by a burn spot on the SIT tube) crossing a light target. One could envision such a maneuver where a lower priority target would cross a higher priority target in an attempt to confuse the tracker. We are using this scenario to confirm applicable portions of the system concept developed in Section 4.2. The sequence of images runs from images 245 through 259; images 250 through 259 are shown in Figures 4.4-1 through 4.4-10.

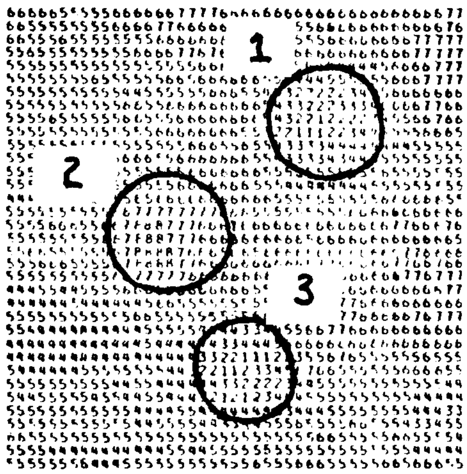

Figure 4.4-1. Image 250

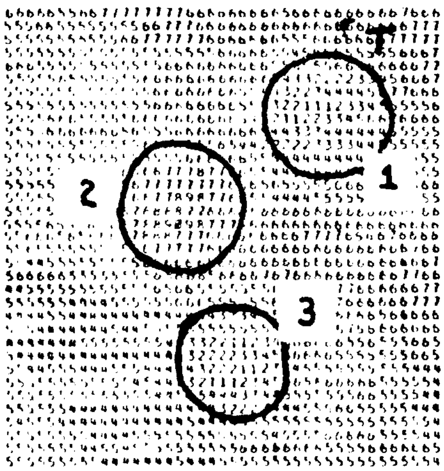

Figure 4.4-2. Image 251

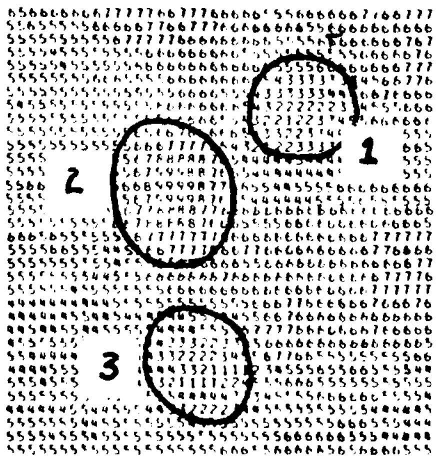

Figure 4.4-3. Image 252

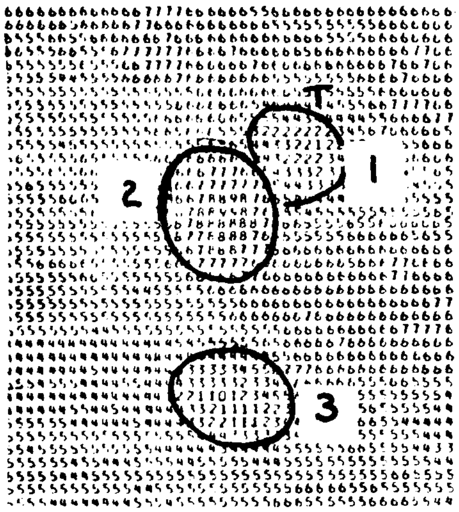

Figure 4.4-4. Image 253

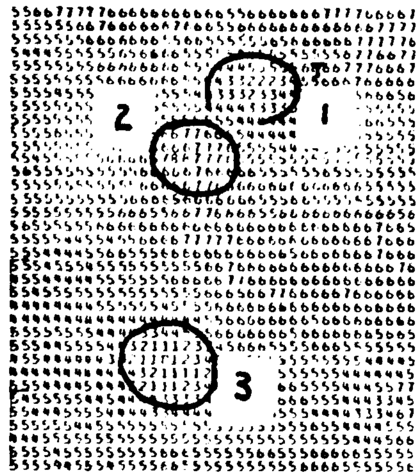

Figure 4.4-5. Image 254

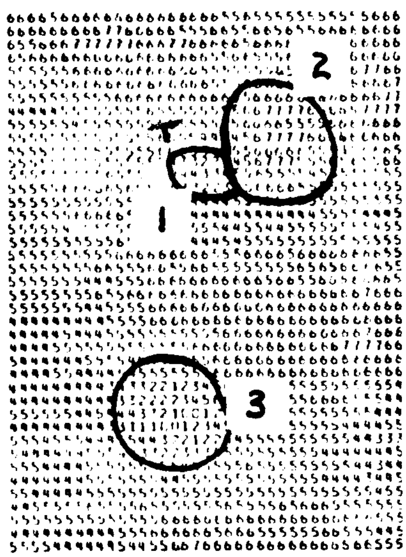

Figure 4.4-6. Image 255

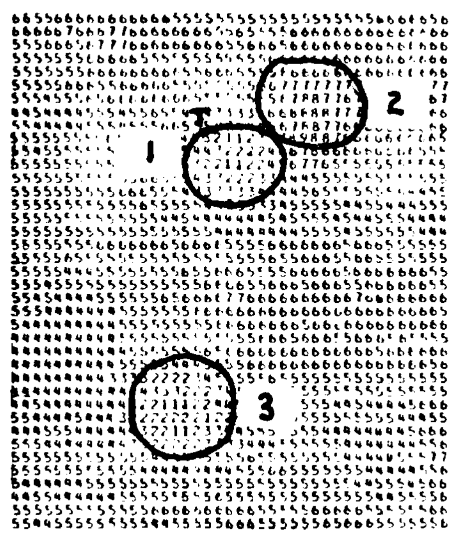

Figure 4.4-7. Image 256

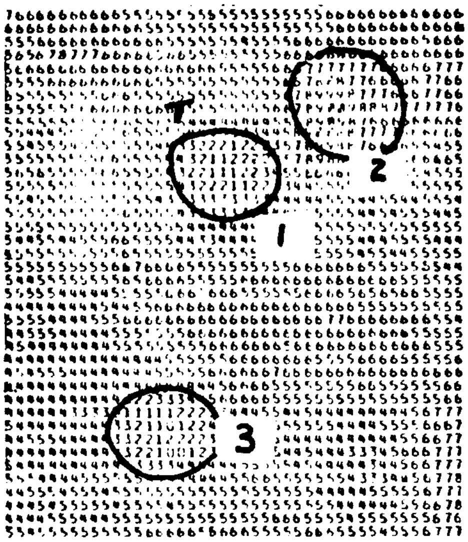

Figure 4.4-8. Image 257

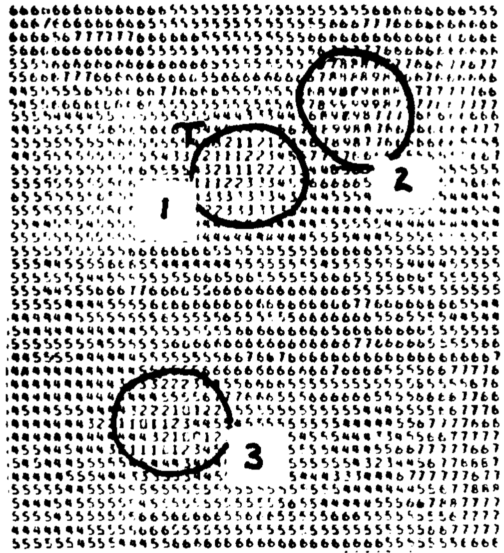

Figure 4.4-9. Image 258

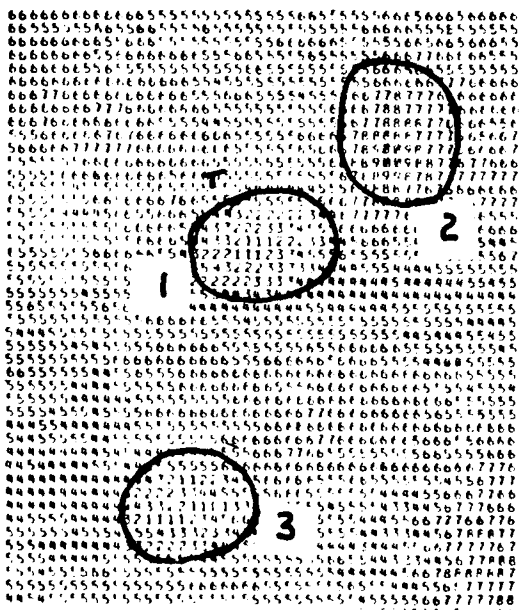

Figure 4.4-10. Image 259

Images 245, 250, and 255 are segmented by the cuer; the intermediate images and images 256-259 are processed by the tracker. Again, the sensor is scanning across the scene, but this time the scan is to the right and up. First, we examine the segmented frames 245, 250, and 255.

There are three targets in the image numbered (1), (2), and (3), shown in Figure 4.4-1. Targets (1) and (3) are sliced at 19 for a maximum number of edge/border matches and target (2) is sliced at 26 for its maximum matches. In image 245, the histogram of the two sectors in front of target (1) are composed of gray levels with values 23-26 but target (2) does not appear in either sector. At image 250, target (1) is sliced at 18, target (3) is sliced at 17, and target (2) is sliced at 27. Image 250, Figure 4.4-1, is interesting because a group of very dark pixels appears in the histogram sectors around target (1). At this point , we know that target (1) may be obscured by the darker region and, therefore, have to be sliced at a higher threshold in the next image. This assumes that it is not completely obscured, in the next cued image. Following the change detection rationale of Section 4.2, we segment the background at a threshold such that the background left is above that of the target in gray scale. This is done because we have a light target with a dark background in the immediate vicinity. Another constraint on the background threshold, of course, is that it obtain a maximum numberof matches on the background. Figure 4.4-11 shows slice thresholds, in image 250, against the number of matches for target (1) and the background. The background is thresholded at 20, and the results are shown in Figure 4.4-12. For image 255, the maximum number of matches on the background are 236. again occuring at a threshold of 20; the result is shown in Figure 4.4-13.

Threshold	Target Matches	Background Matches
16	25	
17	25	
18	→ 28	189
19	28	213
20	28	→ 250
21		215

Figure 4.4-11. Slice Thresholds for Target and Background, Image 250

Superimposed on Figure 4.4-13 are the change results of images 250 and 255. In interpreting change detection results correctly, it is important to anticipate the probable outcome. In this case, we anticipated that target (1) would be obscured; Figure 4.4-13 shows this because half of the hole in the background caused by target (1) is gone. Further , we know that this portion is composed of pixels which have a gray level 20 or higher- not characteristic of target (1) but rather the background. The left portion of the change record , L-shaped, is composed of pixels which are 20; this is conceivably the edge of target (1).

In summary anticipation of an impending darker background should lead to using those portions of the change detection record which are lighter than the background and in the vicinity of the target.

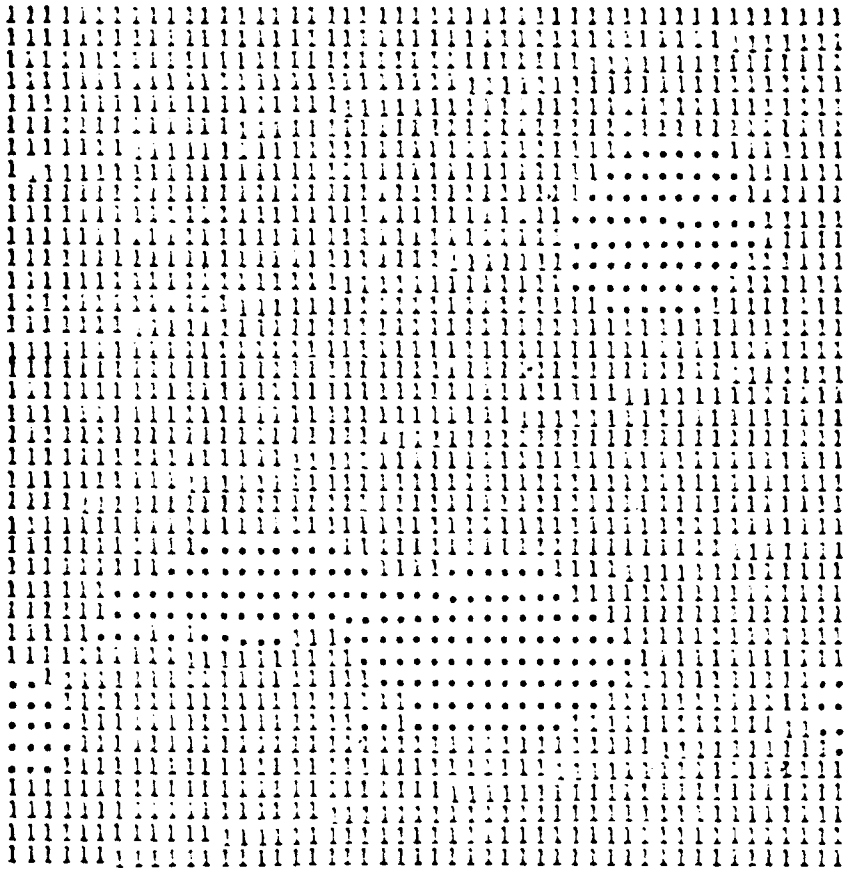

BLOB STATISTICS

Blob	Avg	TOPX	TOPY	BOTX	BOTY	XBAR	YBAR
1. 1	23.26	89	36	89	74	65.22	54.37

BLOB IDENTIFICATIONS

Matches

1. 1 250

Figure 4.4-12. Background of Image 250

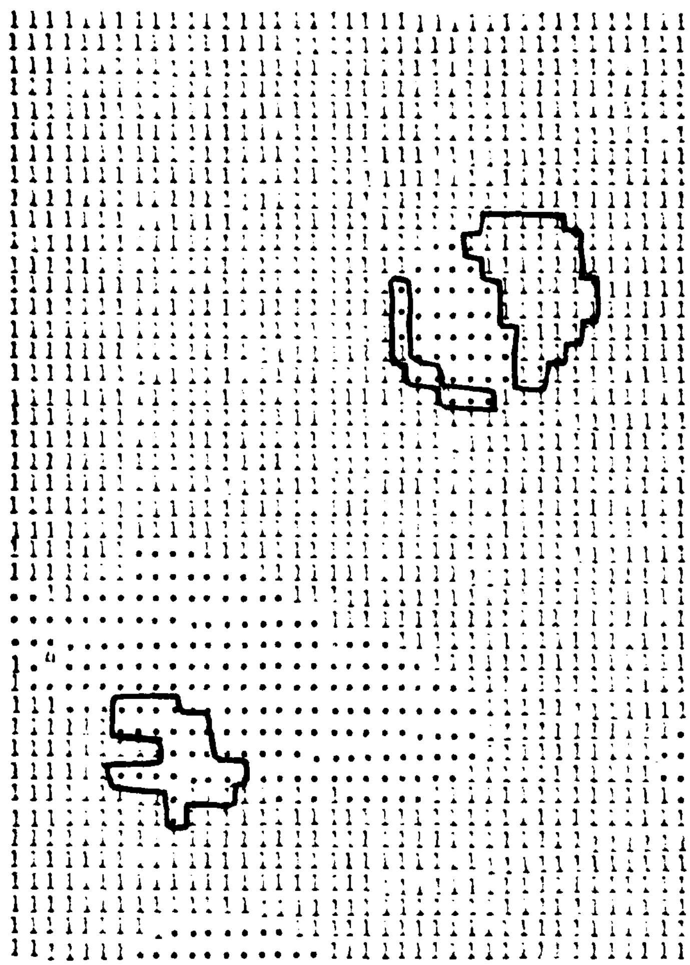

BLOB STATISTICS

	Blob	Avg	TOPX	TOPY	BOTX	BOTY	XBAR	YBAR
1.	1	22.86	72	44	72	96	53.71	63.57
2.	4	20.00	36	73	36	73	36.00	73.00

Figure 4.4-13. Background of Image 255

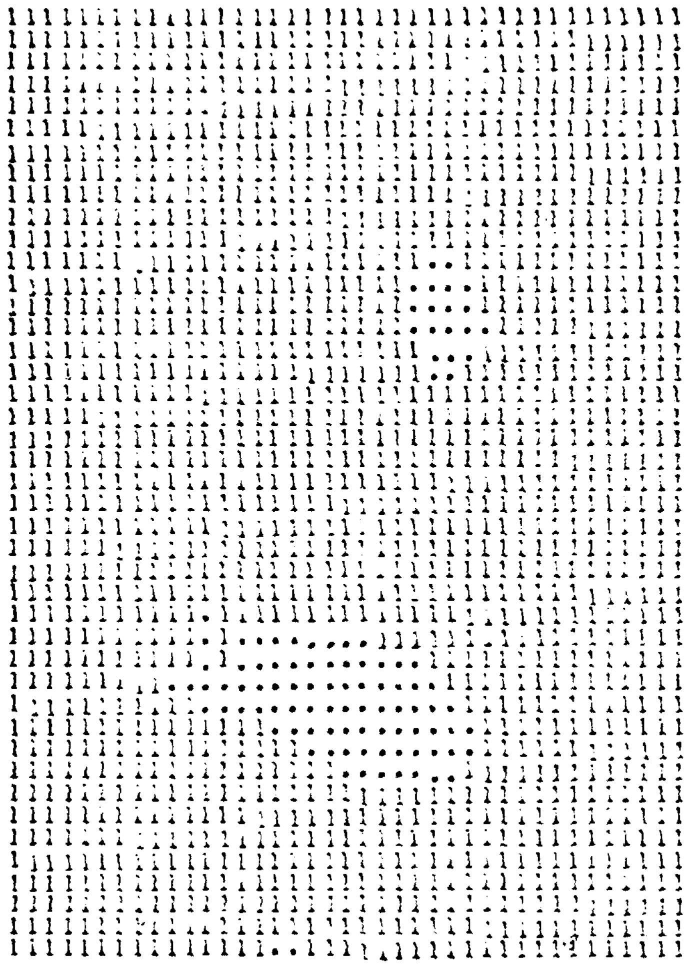

Figure 4.4-14. Direct Segmentation, Image 255

Direct segmentation of image 255 leads to the target image shown in Figure 4.4-14. In this case, the target was almost stationary and was crossed by a dark object. Change detection was not appropriate because there was little change with respect to the background. Since the target was only partially obscured, Figure 4.4-14 shows the unobscured portion which can be used for the track reference window.

In conclusion, change detection and direct segmentation are complementary processes for obscuration. When an obscuration is imminent, factors such as whether or not the target is moving, target position, and target polarity with respect to the impending obscuration provide same heuristics for predicting and interpreting the changes in target signatures.

4.5 DISAPPEARING TARGET NO. 2

This is the second example of a target completely disappearing into heavy clutter where no portions of it are visible as it moves through the clutter. The purpose of analyzing the sequence is to confirm the disappearance using a comparison between the superslice threshold and the average gray level across the histogram of the target. Approximately every tenth frame is sampled and segemented. The results are shown in Figure 4.5-1 for images 303 through 351. Note that the average gray scale $\overline{GL}$ begins to approach

IMAGE

	303	313	323	331	341	351
SuperSlice Threshold, T	19	20	21	20	No Target Segmented.	
Average Gray Level, $\overline{GL}$	17.36	18.95	20.7	20		

Figure 4.5-1. Comparison of Superslice Threshold vs. Average Gray Level

the superslice threshold, T, at image 313 and is within .5 of T at image 323. A difference of .5 in the previous example indicated a target loss. Image 331 offers more evidence of a target loss which is confirmed in images 341 and 351. Figures 4.5-2, 3, ... 7 show images, median filtered, 303, 313, 323, 331, 341, and 351 respectively for the target and a small region around it.

In conclusion, it appears that a comparison of the average gray level across the target, $\overline{GL}$, with the superslice threshold, T, can be used in detecting the presence or absence of a target.

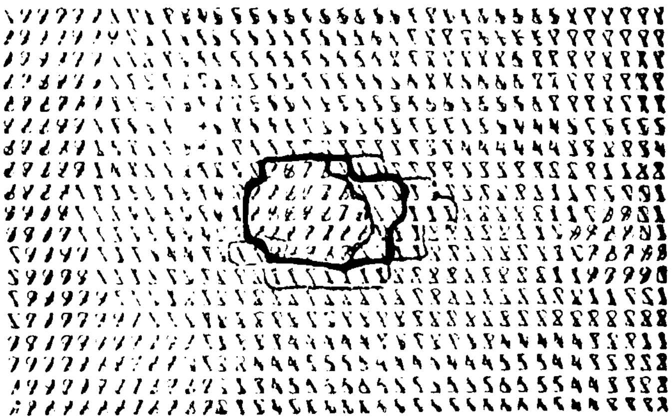

Figure 4.5-2. Image 303

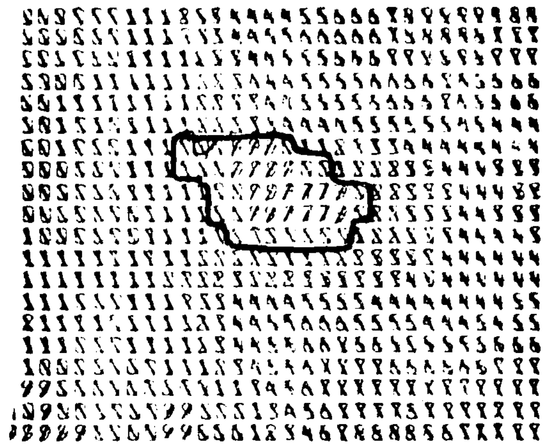

Figure 4.5-3. Image 313

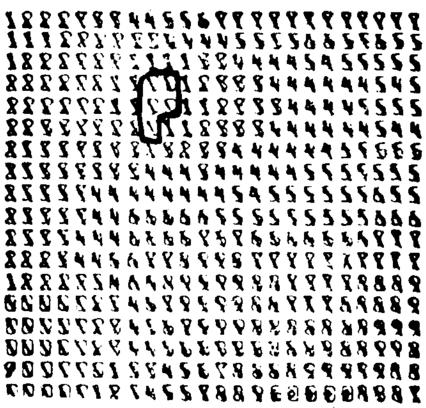

Figure 4.5-4. Image 323

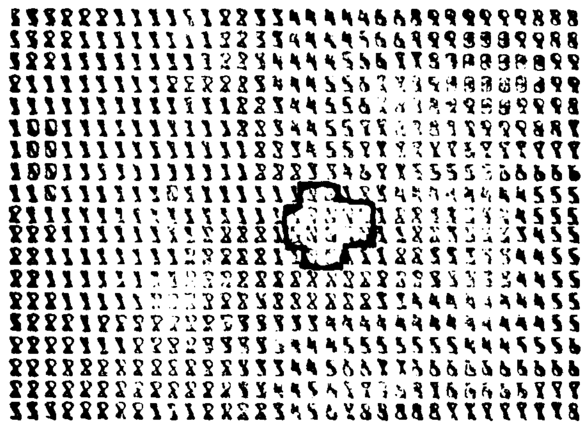

Figure 4.5-5. Image 331

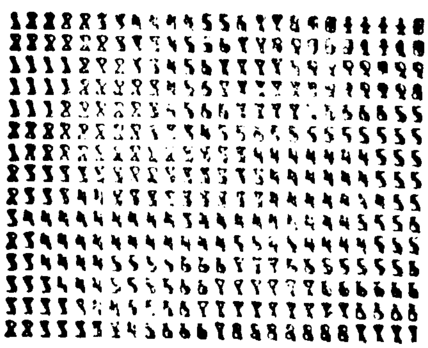

Figure 4.5-5. Image 341

Figure 4.5-6. Image 351

4.6 REAPPEARING TARGET

In Sections 4.3 and 4.5 we analyzed disappearing target examples and provided several techniques for the prompt discovery of a disappearance. It was felt that prompt discovery will give the cuer an advantage by obtaining a reference scene without the target. Then some form of change detection may be employed to test for the reappearance of the target. Let us examine this idea by describing a reacquisition scenario.

Assume a target is completely lost in heavy clutter, i.e. it cannot be seen as it moves through the clutter and away from the point of disappearance. This means that the target could move in any direction from the point of disappearance and subsequently reappear in a partially occluded condition. Further, the target can reappear as a light target against a dark background or vice versa. In particular, the target could reappear at the edge of a light clearing as a slightly darker, partially obscured target. The problem is further compounded by allowing the sensor platform to change range and aspect to the last target position between disappearance and reacquisition. Consider the complications this situation creates for binary change detection employed in earlier examples.

To perform binary change detection, the histogram sectors ahead of the target are employed to predict whether the target gray levels will darken or lighten against the new background. Since we do not know where the target will reappear, we cannot know what the new background will be. Further, as the range and aspect change between disappearance and reappearance, certain areas of the background will change shape and gray level. Interpreting these changes becomes more difficult; recall, that binary change detection was used because the parameters of changes (i.e. scale, rotation, aspect, perspective, S/N ratio) were small. Here, that assumption is substantially weakened.

We approach this problem by performing the inverse of the disappearing target example. That is, we require the reappearing target to have a well-defined (maximum) edge/perimeter match as found by superslice and interior highlights as defined by $T-\overline{GS} > .5$. We anticipate that some background objects (clearings) will be segmented but a reappearance of the target in those regions will be detected by changes in the $T, \overline{GS}$ relation. Hence, we need only perform change detection over those areas which can be segmented by superslice.

We start the process just described at image 641. Figure 4.6-1 shows the number of matches at each threshold for a particular blob in image 641. The permissable gray levels are those less than or equal to the threshold, T.

The table entries show the number of edge-perimeter matches at each threshold. The circled entries indicate where two blobs, separate at a lower threshold, merge at a higher threshold. There are three significant blobs in the image, the others do not appear to affect the results. These are shown in Figure 4.6-2, image 641. Blob No. 7 is the disappearing target and marks the position where the target disappears, Blob No. 5 is a clearing in the woods directly in the path of the disappearing target, and Blob No. 8 represents another clearing in the woods where the target reappears. The remainder of the images 647-667 depict essentially the same scene except the range to target is approximately halved and there is a downward displacement of approximately 50 pixels. Figures 4.6-3, 4, 5, and 6 represent the results of thresholding for images 647-662. In general, these results do not indicate the presence of a target. More specifically, the number of matches do not reach a maximum for the blobs in the series of images. The range of thresolds explored is 10-20. Figure 4.6-7 shows the threshold series for Blob 5 and 8 only. Blob 7 has not segmented as a target since the time that the target disappeared there. The target first reappears at image 657 at the position of Blob 8, however, according

to Figure 4.6-7, there is no target detection. That is, the number of matches does not reach a maximum. Starting at image 662, there is a detection and in images 666 and 667. Note the circled maxima. There is a false detection on Blob 5 at image 657 which is not repeated in the later images. At image 668, the sensor slews and moves the target out of the window being used for frame grabbinb, so image 667 represents the end of file. For images 662, 666, and 667, we compare the superslice threshold against the average gray level over the target in the next step in the detectionprocess in Figure 4.6-8. Hence, the second criterion in the detection process is met for Blob 8. The present approach has the added feature that it is a by-product of the cueing process and several more fairly simple calculations used in detecting a disappearing target. As a matter of fact, the same hardware is used in the disappearing and reappearing cases with one algorithm being the inverse of the other. Recall, that in the disappearing target case maxima were achieved and T-$\overline{GL}$ was used to detect the absence of a target. It should be noted that Blob 5, the clearing in the extrapolated path of the target had T-GL >.5 at several of the intermediate frames between 641 and 667, but achieved a maximum in edge-perimeter match only on one image. In other words, a persistence criterion can be employed to strengthen the validity of the detection.

Figures 4.6-9, 10, 11, 12, 13 shows the clearing as Blob No. 8 for images [illegible]7, 662, 666, and 667. Note, again, that the target reappears at image 657.

In reviewing this work John Dehne, NV&EOL, suggested a conceptual framework for the effort.

From the above discussion it should be obvious that none of the simple target signature based techniques discussed so far (e.g. segmentation and pattern recognition, frame-to-frame tracking, local area change detection) nor their synergistic use is capable of providing a solution to the problem of the re-

appearing target. The difficulty arises from the very close interaction of the target with the background in this case. In previous cases (e.g. crossing object cases, road crossing case) this problem could be overcome by using simple change detection since the target/background interaction took place over a short span in both space and time - which allowed us to avoid a detailed analysis of the background character by assuming that the background (whatever it was) was quasi-static. In the reappearing target case, the target/background interaction takes place over longer spans in both time and space and quasi-static assumptions cannot be expected to apply.

What is needed is a rudimentary theory or model of the anticipated characteristics of both targets and backgrounds. Fortunately, the work to date suggests a basis for such a mode. We have noted that the disappearance of a target is detectable both as the failure of superslice to find it (e.g. inability to find a maximization of edge/border point matches with threshold variation) and by the loss of interior detail in the target just prior to disappearance. This would suggest the following basic models.

TARGET MODEL: Targets are man-made objects. As objects they are of limited spatial extent and are composed of "blobs" which "move together" in time and space. As man-made artifacts they are surrounded by well-defined edges/borders and contain significant interior detail.

BACKGROUND MODEL: Backgrounds are composed of objects (man-made and natural) and regions. Objects (e.g. roads. clearings) are of limited spatial extent (in at least one direction) and tend to be bounded by well-defined edges/borders. They do not change over reasonable time spans. Regions are areas of large spatial extent, generally relatively uniform in intensity or texture and often having poorly defined edges/borders".

IMAGE 641

MATCHES AT THRESHOLD

BLOB NO.	10	11	12	13	14	15	16	17	18	19	20	21	22
1					5	12	19	25	121	140	154		
2				1	18	30	42	46	2				
3					3	1							
4							11	30	3				
5							1	4	6	8	13		
6									9	4			
7									12	27	129		
8									7	17	24		
9										3	24		
10										3	19		
11										5	5		
12										24	6		
13										3	7		
14											7		

1 Blob 3 merges into Blob 2
2 Blob 2 merges into Blob 1
3 Blob 4 merges into Blob 1
4 Blob 6 merges into Blob 1
5 Blob 11 merges into Blob 7
6 Blob 12 merges into Blob 7
7 Blob 13 merges into Blob 7

Figure 4.6-1

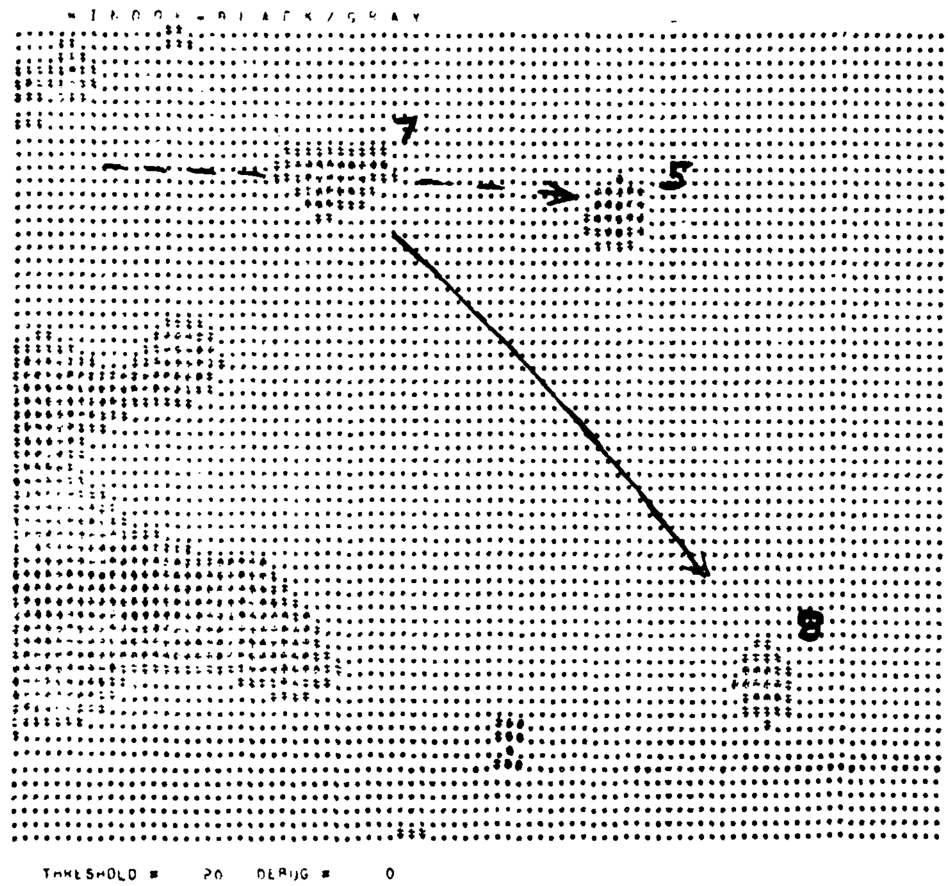

Figure 4.6-2, Image 641

IMAGE 647

MATCHES AT THRESHOLD

BLOB NO.	10	11	12	13	14	15	16	17	18	19	20	21	22
1						3	14	77	127	130	253		
2				1	34	43	47	2					
3					1								
4							10	22	3				
5							3	7	10	18	25		
6									12	6			
7									2	32	253		
8									2	12	19		
9											9		
10										3	37		
11									3	5			
12									5	49	7		
13										4			
14											8		
15										5	10		
16										1	11		
17										2	12		

1 Blob 3 appears merged in Blob 2 from the beginning
2 Blob 2 merges into Blob 1
3 Blob 4 merges into Blob 1
4 Blob 13 initially appears already merged into Blob 12
5 *Blob 11 merged into Blob 12*
6 Blob 6 merged into Blob 1
7 Blob 12 merged into Blob 7
8 Blob 14 initially appears already merged into Blob 12
9 Blob 9 initially appears already merged into Blob 10
10 Blob 15 merged into Blob 7
11 Blob 16 merged into Blob 7
12 Blob 17 merged into Blob 7

Figure 4.5-3

IMAGE 652

MATCHES AT THRESHOLD

BLOB NO.	10	11	12	13	14	15	16	17	18	19	20	21
1					6	14	20	2				
2			1	20	37	41	56	104	128	129	144	
3				1								
4						1	13	3				
5							1	4	6	12	13	
6								6	4			
7										15	104	
8									11	24	28	
9										11	46	
10											10	
11									11	6		
12									1	60	8	
13									6	7		
14											7	
15										5	8	
16											1	
17												
18											2	
19											0	

1 Blob 3 initially appears already merged into Blob 2
2 Blob 1 merges into Blob 2
3 Blob 4 merges into Blob 2
4 Blob 6 merges into Blob 2
6 Blob 11 merges into Blob 12
7 Blob 13 merges into Blob 12
8 Blob 12 merged into Blob 7
9 Blob 15 merged into Blob 7
10 Blob 10 initially appears merged into Blob 9

Figure 4.5-4

IMAGE 657

MATCHES AT THRESHOLD

BLOB NO.	10	11	12	13	14	15	16	17	18	19	20	21
1												
2				1	14	23	58	55	60	97	191	
3												
4					5	10	1					
5						5	7	15	17	20	29	
6												
7										53	3	
8								8	19	26	30	
9									4	19	60	
10									2	2		
11												
12												
13												
14										8	13	
15												
16						5	14	24	30	3		
17												
18												
19										11	28	
20										4	4	

1 Blob 4 merges into Blob 2
2 Blob 10 merged into Blob 9
3 Blob 16 merged into Blob 2
4 Blob 20 merged into Blob 9
5 Blob 7 merged into Blob 2

Figure 4.5-5

IMAGE 662

MATCHES AT THRESHOLD

BLOB NO.	10	11	12	13	14	15	16	17	18	19	20
1											
2				8	23	36	79	77	135	226	268
3											
4					6	20	1				
5					6	6	10	15	18	20	28
6											
7											
8								6	16	28	33
9										28	5
10										21	6
11											
12									61	4	
13											
14										7	15
15											
16							11	2			
17											
18											
19										10	23
20											
21							2	38	3		

Blob 4 merged into Blob 2
Blob 16 merged into Blob 21
Blob 21 merged into Blob 2
Blob 12 merged into Blob 2
Blob 9 merged into Blob 2
Blob 10 merged into Blob 2

Figure 4.5-6

Threshold Down	Blob 5 (641)	Blob 8 (641)	Blob 5 (647)	Blob 8 (647)	Blob 5 (652)	Blob 8 (652)	Blob 5 (657)	Blob 8 (657)	Blob 5 (662)	Blob 8 (662)
16	6	0	17	0	5	0	12	0	10	0
17	8	0	19	0	9	0	21	0	12	0
18	12	17	21	8	14	20	24	22	17	26
19	16	25	23	15	20	34	21	27	23	27
20	19	32	27	31	25	39	24	29	28	23
21	24	29	29	40	27	53	49	33	29	merged
22	26	60	merged		merged		merged			
23										
24										

Threshold Down	Blob 5 (666)	Blob 8 (666)	Blob 5 (667)	Blob 8 (667)
16	18	0		
17	21	20	12	0
18	26	32	17	26
19	28	36	23	26
20	32	34	28	23
21	35	merged	29	out of window

Figure 4.6-7 Threshold Down

	IMAGE		
	662	666	667
Superslice Threshold, T	GL<19	GL<19	GL<18
Average Gray Level, GL	17.6	17.37	17.00

Figure 4.6-8. Comparison of Superslice Threshold and Average Gray Level

Figure 4.6-9 Blob 8,
Image 652

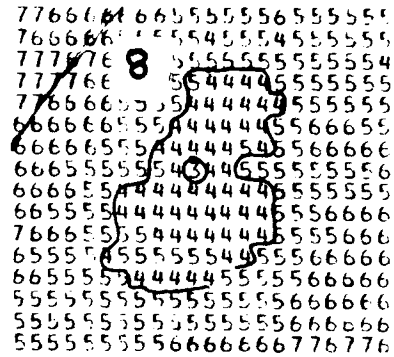

Figure 4.6-10 Blob 8,
Image 657

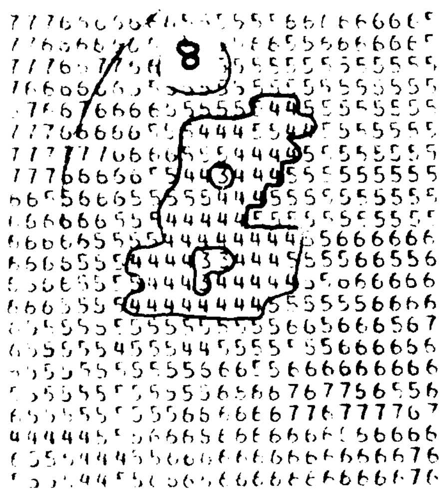

Figure 4.6-11 Blob 8,
Image 662

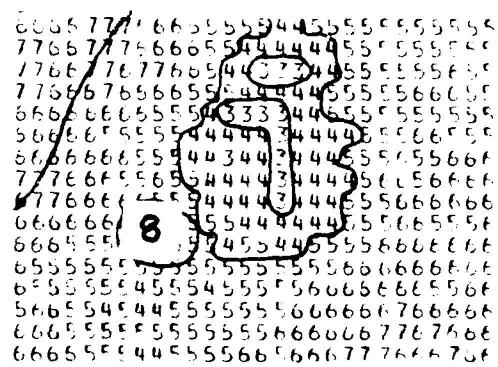

Figure 4.6-12 Blob 8,
Image 666

AD-A082 183   WESTINGHOUSE DEFENSE AND ELECTRONIC SYSTEMS CENTER B--ETC F/G 17/7
INTELLIGENT TRACKING TECHNIQUES.(U)
JUL 79 T J WILLETT, J ROMANSKI, J SHIPLEY   DAAK70-78-C-0167

UNCLASSIFIED   NL

2 of 2

END
DATE
FILMED
4-80
DTIC

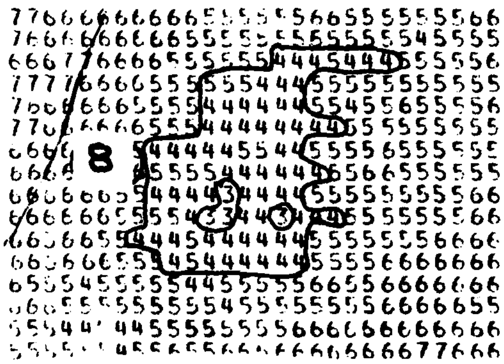

Figure 4.6-13 Blob 8,
Image 667

4.7 THREE CROSSING TARGETS

This scenario was described in Section 4.0 of the Second Quarterly Report. An APC is crossing between two other APC's; all the targets are light and the background is dark. There is no gray level differentiation between the three targets shown in Figure 4.7-1. We described the idea of tracking the bottom

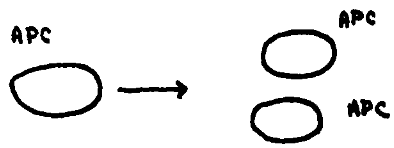

Figure 4.7-1. APC Passing Between Two Other APC's

and top y coordinates of all three targets to maintain track. Here, in an effort to have a single algorithm handling signature prediction problems, we apply the change detection technique discussed in Section 4.2 (Road Crossing Case) of this report. We present a heuristic analysis of this approach.

The histogram, moving ahead of the left-most APC, would detect the presence of similar gray levels in the two targets on the right. Recall, there is a histogram analysis performed on the background just ahead of the target. The position of the histogram is derived from the track window position errors. We perform change detection by segmenting the background and, in the process of doing this, the two APC's would be described as "holes" thus confirming their approximate positions. Recall also, that segmenting a dark background means we are slicing downward from high gray levels. When the targets merge, the image looks like Figure 4.7-2. That is, there is considerable "bridging"

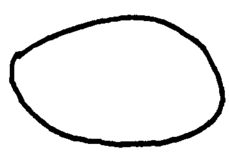

Figure 4.7-2. Merged Targets

among the targets. The binary change detection record, thresholded at the maximum number of matches on the background, between Figures 4.7-1 and 4.7-2 is shown in Figure 4.7-3. In interpreting Figure 4.7-3, it is important to understand where a light region has been added or deleted. The cross-hatched area, , means that the area is dark in the second record; the area denoted by the parallel slanted lines, , means that this light area is present in the second record. Hence, the target of interest must be in this new light area somewhere. The first image, 4.7-1, is now replaced in memory

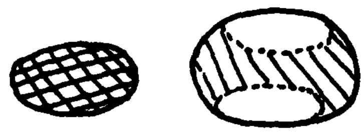

Figure 4.7-3. Change Detection Record

by the second image, Figure 4.7-3. The final image appears in Figure 4.7-4 and is the mirror reflection of Figure 4.7-1. The change record between Figure 4.7-2

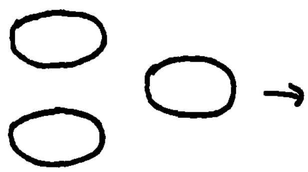

Figure 4.7-4. Completion of Crossing

and Figure 4.7-4 is shown in Figure 4.7-5. This time the dark region, , is between the two stationary targets. And the new light region in the second image is the crossing target, which has now passed beyond the other two.

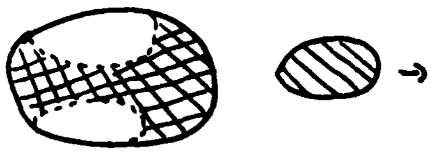

Figure 4.7-5. Change Detection Record

In conclusion, the same approach is applied to both the Road Crossing Case and the Three Crossing Targets Case. Also, in both cases, the tracker is shifted to the unobscured rear of the crossing target until it disappears and/or the front portion when it reappears.